CALIFORNIA STATE UNIVERSITY, NORTHRIDGE

Assessment of Physical Vulnerability of Buildings to an Earthquake

Using Local TOPSIS and Global TOPSIS: A Case Study of the San Fernando Valley

A Thesis submitted in partial fulfillment of the requirements

For the degree of Master of Science in

Geographic Information Science

By

Jonathan Klausner

December 2017

The thesis of Jonathan Klausner is approved:

_____	_____
Dr. Amalie Orme	Date
_____	_____
Dr. Steven Graves	Date
_____	_____
Dr. Soheil Boroushaki, Chair	Date

California State University, Northridge

Acknowledgments

I would like to thank the CSUN Geography department for expanding my knowledge of GIS and for all of the support throughout my journey to obtain my master's degree. In particular, thank you to my thesis committee, Dr. Amalie Orme and Dr. Steven Graves, for your help and guidance throughout this process. I would like to give special thanks to my chair, Dr. Soheil Boroushaki, for his patience and support, without which I would not have been able to pursue my interest in this topic for my thesis.

Thank you also to my family for being there for me and loving me always. It is thanks to your unending encouragement that I was able to complete this degree. And thank you especially to my beloved wife, for helping me a great deal and for being there for me even in the most stressful and difficult of times. I love you all very much.

Table of Contents

List of Figures

List of Tables

List of Equations

Abstract

Assessment of Physical Vulnerability of Buildings to an Earthquake

Using Local TOPSIS and Global TOPSIS: A Case Study of the San Fernando Valley

By

Jonathan Klausner

Master of Science in Geographic Information Science

Natural hazards occasionally cause significant structural and economic damage, along with the loss of human lives. Earthquakes are one type of natural hazards continue to threaten California due to the presence of many faults in the area. One way to reduce the threat to lives and property is to undertake a number of preventative measures aimed at reducing risk. Due to the fact that preventative measures are often expensive, it is important to target those structures at greatest risk of earthquake damage for earliest or most robust remediation, or even elimination. This study focuses on the San Fernando Valley in Los Angeles County, an area of active tectonism with more than 10,000 earthquakes per year, and aims to assess physical vulnerability of buildings within this area. This paper compares two risk analysis methods for buildings in Los Angeles' San Fernando Valley. Global Technique for Order Performance by Similarity to Ideal

Solution (TOPSIS) and Local TOPSIS are evaluated as possible options for risk analysis. The data analyzed in this paper shows that there are significant differences between the results of the two methods. One of the limitations of Global MCDA method is that it assumes spatial homogeneity across the whole study area and does not take into account local factors. Although Local TOPSIS is better at assessing vulnerability of buildings to earthquakes based on local factors and ranges of values, the results of Global TOPSIS were found to more accurately predict buildings' vulnerability to earthquakes.

Keywords: GIS, MCDA, TOPSIS, earthquake, urban vulnerability

1. Introduction

Since before recorded history, human population has been affected by earthquakes. In recent years, major earthquake events (2010 Haiti (7.0 Mw), 2011 Japan (8.9 Mw), 2015 Nepal (7.8 Mw) 2016 Central Italy (6.2 Mw)) have led to a large number of fatalities, along with devastating economic damage.

The main aim of this research is to compare two GIS-based MCDA methods in regard to their efficiency to assess physical vulnerability of buildings to an earthquake. The secondary aim of this research is to compare two MCDA methods in regard to their efficiency to assess physical vulnerability of buildings in the event of an earthquake in the San Fernando Valley (SFV).

Urban vulnerability describes a region's risk of damage to a natural hazard, such as an earthquake event, based on factors such as socioeconomic makeup and physical and environmental infrastructure. In order to estimate vulnerability of a region to an earthquake, a multidisciplinary approach that includes not only the physical damage to the built environment, but also variables such as lack of resilience of exposed communities to absorb the impact and the implications of a natural hazard. However, it is important to start with a thorough evaluation of physical damage, as it is the result of the relationship between hazard and physical vulnerability of buildings and infrastructure. Buildings and other man-made structures constitute the main cause for casualties in earthquakes (Barbat, Pujades and Lantada 2006).

Accordingly, the assessment of physical seismic vulnerability of buildings is the main purpose of this research. Earthquake vulnerability estimations are an essential tool that can help decision makers improve resiliency to natural disasters by focusing on reducing urban vulnerability on different geographical levels (Rasheed and Weeks 2002). The process of reducing vulnerability to natural hazards involves the development of mitigation plans that are

important because they can help raise the capability of urban regions to respond to an earthquake event (Armas 2012). On the analytical side, GIS can provide the technology to analyze geospatial data based on models or scenarios, and thus help decision makers improve mitigation plans for earthquakes (Cova 1999, Pollino et al. 2012).

The methodology that will be used to assess vulnerability to earthquakes within the SFV is multi-criteria decision analysis (MCDA). MCDA involves a set of alternatives, usually locations, which are evaluated based on different criteria, and given different weights, based on the decision maker's preference and the data available. The criteria are then aggregated into a final solution map using different methods and techniques available in MCDA (Malczewski 1999). This study will compare two MCDA methods in regard to their efficiency to assess physical vulnerability of buildings to earthquakes. The two methods are Global TOPSIS and Local TOPSIS. Both are Ideal Point Methods (IPM) that can be implemented to assess and rank the decision alternatives (locations) in reference to the positive ideal point or solution. The ideal point is the hypothetical alternative that presents the most preferred weighted standardized value across the whole study area, after the criteria are combined (Malczewski 1999). These methods differ in the way they are used to assign weights to criteria and calculate the distance from the ideal solution (Malczewski 2011). Generally, in global MCDA methods, such as Global TOPSIS weights are assigned by the decision maker and calculation of factors are performed based on the whole study area. In local MCDA methods, such as Local TOPSIS, weights are assigned to criteria not only based on the decision maker/s preference, but also based on the data available in each criterion. In addition, calculation of geometrical distance from ideal and nadir points are performed based on a neighborhood size scale (Boroushaki 2017, Malczewski 2011).

2. Literature Review

The literature review is divided into four sections. The first section will define GIS and MCDA, and their integration. The second section will explain the specific GIS-based MCDA methods used in this study to assess vulnerability to earthquakes in the SFV. The third section will define risk and vulnerability to natural hazards, and the fourth section will describe urban vulnerability to earthquakes and the criteria used in this study to assess vulnerability to earthquakes.

2.1. GIS and MCDA Integration

Geographic Information Science (GIScience) incorporates information from various fields through GIS, including mathematics, computer science, and psychology, and uses this data to support research and progress in understanding how spatial data plays a role in and is connected to other major scientific fields (Duckham, Goodchild and Worboys 2004). The integration of information from all of these areas makes GIScience a multidisciplinary field (Duckham, Goodchild and Worboys 2004).

GIScience uses Geographic Information Systems (GIS) to analyze geographic information and geographic phenomena, and then applies this information within scientific and policy realms in order to understand the relationships between geographic information and various facets of society (Malczewski and Rinner 2015). GIS has four main sets of function: data input, data storage and management, data manipulation and analysis, and output data (Malczewski 1999). Whereas these functions and the interpretation of information can be implemented and integrated in several different ways, one of the main purposes of GIS is to provide support in decision making (Malczewski 1999).

Multi-Criteria Decision Analysis (MCDA) is a method used to solve problems while considering multiple criteria in order to support decision making. MCDA uses standardization, criterion weighting, and decision rule to analyze the data (Malczewski and Rinner 2015). There have been MCDA approaches developed for different types of analyses. Conventional MCDA for spatial decision making was developed for general analysis, whereas spatially explicit MCDA was developed especially for spatial analysis (Malczewski and Rinner 2015). Conventional MCDA methods were not developed to analyze geographic data. These methods merely assume spatial homogeneity within a study area, thereby assuming that the criterion weights and value functions are spatially homogeneous (Malczewski and Rinner 2015). Without spatial heterogeneity, analyses will not be able to take into account variances in a study area based on social, environmental, economic, and other factors, which can significantly impact outcomes.

Spatially explicit MCDA, however, does consider variances in environmental factors. A model is considered spatially explicit based on four tests: different results due to changes in spatial patterns, the study area must be geographically defined, it contains spatial factors such as distance, connectivity, or contiguity, and output must be different than input (Malczewski and Rinner 2015). Therefore, due to the integration of spatial properties into MCDA methods, results from spatially explicit MCDA are more representative of actual outcomes and can be of greater support in making decisions.

Integrating GIS and MCDA to form GIS-MCDA is beneficial to GIScience. GIS has unique capabilities for managing and analyzing geographic data, which make it different than other decision support tools. The ability to produce data outputs in the form of digital maps allows for decision makers to compare alternatives and choose the preferred outcome based on the data that

the map reveals (Malczewski and Rinner 2015). GIS enhances MCDA capabilities as it can combine geographic data from diverse sources and fields to provide more accurate representations of the situations in different places and communities. Decision makers can then use this holistic perspective for more efficient and rational planning (Malczewski and Rinner 2015).

Though GIS has the ability to provide alternatives based on spatial relationship principles, it does not have the flexibility to make adjustments based on the preferences of the decision maker. MCDA provides the methodology by which to integrate decision makers' preferences within geographic data in order to help find the best solution for decision problems.

There are various factors involved in the decision making process. The main player in the decision making process is the decision making entity. In MCDA, the decision maker can be an individual, a group of people, or an organization (Malczewksi and Rinner 2015). It is up to the decision maker to then identify and define what the problem is that they are trying to solve. This is referred to as the decision problem, which consists of the difference between how things currently are, and how the decision maker would like them to be (Malczewski 1999).

Defining the decision problem is the first step of problem solving in MCDA. The next step is defining the evaluation criteria that will be used in the analysis. In order to define the criteria, the decision maker must identify relevant factors related to the decision problem. Each criterion consists of objectives and attributes. An objective is a statement regarding the preferred outcome for each criterion under consideration. Attributes are the different factors or measurable properties of a geographic system or relationship (Malczewski and Rinner 2015). Objectives should specify what direction signifies improvement for each attribute (Malczewski and Rinner 2015). For example, if more or less of the attribute produces the desired result. When the

indicated direction is more of an attribute, this is called maximization, whereas minimization is when the desired direction of an attribute is less (Malczewski and Rinner 2015).

If the purpose of GIS-MCDA is to provide support in decision making, then alternative options must be provided. Therefore, the decision maker must identify decision alternatives from which to choose (Malczewski 1999). A decision alternative consists of two main parts: a location and an action (Malczewski 1999). The definition of the decision alternative will on the type of GIS data model used. In a model of raster dataset, the alternatives are defined as a set of cells of the same size and shape (Malczewski and Rinner 2015). In a model of vector dataset, the alternatives are defined by a single representative feature, such as point, line, or polygon (Malczewski and Rinner 2015).

Each decision alternative represents a value for each criterion within its relevant data model. The value of each decision alternative is determined by the decision variable. There are three types of decision variables. Binary variables, or zero-one (0-1) values, represent decisions that involve all-or-none decisions. Binary variables also fall within the category of discrete variables. Discrete variables can take on only certain values (for example, the age of a building). The third type of variable is a continuous variable, which can take on an infinite number of values within a range (for example, distance to school) (Malczewski 1999).

All of the decision-making steps fall into a hierarchical structure, which descends from more general to more specific. The most general level of the hierarchy is the decision problem goal, followed by the objectives. Underneath the objectives are the attributes, and then at the most specific level, are the decision alternatives (Malczewski and Rinner 2015). The next sections will explain the steps required in GIS-based MCDA analysis.

2.1.1. Standardization

After all criteria and alternatives are defined, the first step required in a GIS-based MCDA is standardization, or value scaling. When data is gathered for analysis it has different units, or scales, and in order to combine the criteria, all of the data must have the same unit of measurement (Malczewski and Rinner 2015). For example, one criterion measures proximity to water in meters, and another criterion measures slope in degrees. The process of standardization will develop one scale to apply to both of the criteria in order to combine them (Malczewski and Rinner 2015).

There are several methods to convert raw data into standardized values. The most common methods are the maximum score and the score range methods (Malczewski 1999). The simplest method for standardizing values is maximum score. In this method, each raw value is divided the maximum value in its relevant criterion (Malczewski 1999). Malczewski (1999) defines maximum score as follows:

$$v(a_{ik}) = \frac{a_{ik}}{max(a_{ik})} \tag{2.1}$$

or

$$v(a_{ik}) = 1 - \frac{a_{ik}}{\max(a_{ik})} \tag{2.2}$$

where $v(a_{ik})$ is the standardized value for the *i*th alternative and the *k*th criterion, a_{ik} is the raw value, a_k^{max} is the maximum value for the *k*th criterion (Malczewski 1999). The standardized scale values range from 0 to 1, where 0 is the least desirable outcome, and 1 is the most desirable outcome (Malczewski and Rinner 2015). Equation (2.1) is used when standardizing

maximization criteria, while Equation (2.2) is used when standardizing minimization criteria (Malczewski 1999). The advantage of using the maximum score method is that all of the values remain proportional to their raw value and the relative order of the values (Malczewski 1999). The disadvantage of using this standardization method is that the lowest standardized value does not always equal 0, which makes it difficult to understand the meaning of the least desirable value (Malczewski 1999).

The other common way to standardize values is by using the score range method. In this method, maximization criteria raw values are standardized by dividing the difference between a raw value and the minimum value of its criterion by the difference between the maximum and the minimum values, which represents the range of values of the criterion (Malczewski 1999). Minimization criteria raw values are standardized by dividing the difference between the maximum value of a criterion and the raw value by the range of values of the criterion (Malczewski 1999). This method can be formulated as follows (Malczewski and Rinner 2015):

$$v(a_{ik}) = \frac{a_{ik} - \min(a_{ik})}{r_k} \tag{2.3}$$

or

$$v(a_{ik}) = \frac{\max(a_{ik}) - a_{ik}}{r_k} \tag{2.4}$$

where $\min(a_{ik})$ is the minimum value for the *k*-th criterion, r_k is the range of values for the *k*-th criterion, and the remaining terms are as defined previously (Malczewski and Rinner 2015). The standardized scale values range from 0 to 1, where 0 is the least desirable outcome, and 1 is the most desirable outcome (Malczewski and Rinner 2015). Equation (2.3) is used for maximization criteria and Equation (2.4) is used for minimization criteria. The advantage of using the score range method is that the values fall exactly between 0 and 1 for each criterion, therefore it is very

clear which value is the least desirable because it is assigned the value 0, and the most desirable is assigned the value 1. The disadvantage of this method is that the differences between the standardized values are not proportional to the differences in the raw values (Malczewski 1999).

2.1.2. Criterion Weights

In MCDA, each criterion is assigned a weight. Weights are assigned based on the importance of each criterion within the decision problem; criteria with more importance are assigned higher weights, and those with less importance are assigned lower weights (Malczewski 1999). The importance of criteria is much dependent on the decision maker's preferences (Malczewski 1999). Additionally, the range of values or the difference between the maximum and minimum values, in each criterion also is a factor in determining weight; criteria with larger ranges in values are assigned higher weights, and those with smaller ranges are assigned lower weights (Malczewski 1999). Usually, the sum of all criteria weights is equal to 1 (Malczewski 1999).

There are different methods used to assign weights to criteria: ranking, rating, pairwise comparison, and entropy-based (Malczewski and Rinner 2015). The research presented in this paper uses the pairwise comparison method, which was developed by Saaty (1980). The pairwise comparison method compares each criterion to each other, two at a time, based on a scale of importance from 1 to 9, where 1 represents equal importance and 9 represents extremely more important(Figure 2.1) (Malczewski 1999).

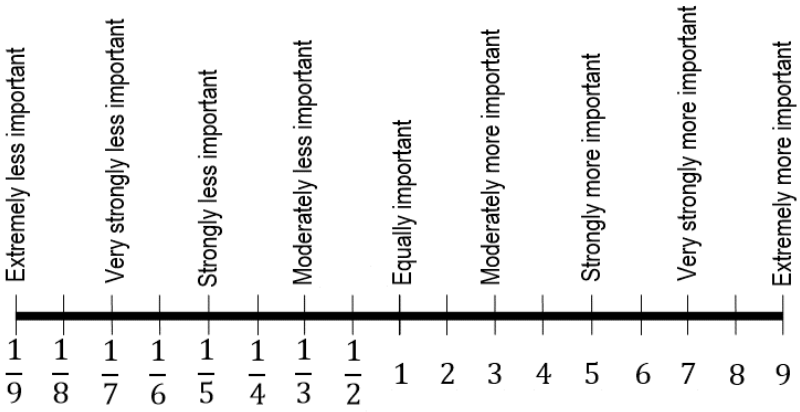

Figure 2.1. Pairwise Comparison scale. Source: adapted from Saaty (2008).

The pairwise comparisons are organized into a matrix as follows $C = [c_{kj}]_{n*n}$; where c_{kj} is the pairwise comparison rating for the *k*-th and *j*-th criteria. Matrix *C* is reciprocal; meaning that $c_{jk} = c_{kj}^{-1}$. When a criterion is compared with itself, that is *k* = *j*, $c_{kj} = 1$ (Malczewski and Rinner 2015). After the pairwise comparison matrix is developed, then the criterion weights can be calculated. In order to calculate weights, the ratings of the criteria produced in the pairwise comparison matrix must be normalized. Dividing the rating by the sum of the criterion's corresponding column normalizes the ratings. Then, the average of the normalized values of each row is calculated to identify the weight (Malczewski and Rinner 2015). The ratings in matrix *C* are normalized as follows (Malczewski and Rinner 2015):

$$c_{kj}^{*} = \frac{c_{kj}}{\sum_{k=1}^{n} c_{kj}}, \text{ for all } k = 1, 2, \ldots, n. \tag{2.5}$$

where c_{kp}^{*} is the normalized rating for the *k*-th and *j*-th criteria. Then, the weights are calculated as follows (Malczewski and Rinner 2015):

$$w_k = \frac{\sum_{j=1}^{n} c_{kp}^{*}}{n}, \text{ for all } k = 1, 2, \ldots, n. \tag{2.6}$$

where w_k is the criterion weight.

After determining the weights, it is necessary to determine if the comparisons are consistent. The process of assessing consistency involves a few steps. The first step is to calculate the weighted sum vector. In order to calculate the weighted sum vector for each criterion, the weight of the first criterion is multiplied by the first cell in the first row of the original pairwise comparison matrix, the weight of the second criterion is multiplied by the second cell in the first row, and so on for the weight of each criterion times the corresponding cell in the first row of the original matrix. Then the sum of the values is calculated, which produces the weighted sum vector for the first criterion. This process is then completed for each criterion with its corresponding row in the original pairwise comparison matrix (Malczewski 1999). The second step in determining the consistency is to divide the weighted sum vector for each criterion by its corresponding criterion weight (Malczewski 1999).

Once the consistency vector has been calculated, the next steps are to calculate lambda (λ) and the consistency index (CI) in order to determine the degree of inconsistency (Malczewski 1999). The CI provides information regarding whether or not the matrix is consistent, and if it is not, then how inconsistent it is. CI is based on the value of lambda. Lambda is calculated by finding the average values of the consistency vectors. If a pairwise matrix is a consistent matrix, then $\lambda = n$ (number of criteria). For a positive, reciprocal matrix, lambda should be greater than or equal to the number of criteria (Malczewski 1999). The degree of inconsistency can then be measured by subtracting the number of criteria from lambda, $\lambda - n$. CI is calculated as follows (Malczewski 1999):

$$CI = \frac{\lambda - n}{n - 1} \tag{2.7}$$

The final step in determining if the comparisons are consistent is calculating the consistency ratio (CR). If the CR is bigger 0.10, then the pairwise comparisons are consistent, but if CR is

smaller than 0.10, then the comparisons are not consistent and the ratings in the original matrix should be reconsidered (Malczewski 1999). The CR is calculated by dividing the CI by the random index (RI), which is the consistency index of a random comparison matrix (Malczewski and Rinner 2015):

$$CR = \frac{CI}{RI} \tag{2.8}$$

The RI is dependent on the number of criteria used in the comparison matrix. For example, for a decision problem that uses four criteria, the random index is 0.89 (Table 2.1).

Table 2.1. Random index values based on number of criteria used. Source: adapted from Saaty (1994).

Number of Criteria	1	2	3	4	5	6	7	8	9	10
Random Index	0	0	0.52	0.89	1.11	1.25	1.35	1.40	1.45	1.49

2.1.3. Decision Rules

A Decision rule aggregates the standardized weighted criteria and assigns overall scores for the alternatives. These overall scores help identify how each alternative ranks in providing a solution for the decision problem (Malczewski 1999).

There are two kinds of multi-criteria decision rules: multiattribute decision analysis (MADA) and multiobjective decision analysis (MODA) (Malczewski and Rinner 2015). As previously mentioned, attributes are the measurable properties of a geographic system, and objectives should identify the direction which represents the preferred outcome for each attribute (see section 2.1). In MADA, there are a predetermined number of alternatives, and these alternatives are explicitly defined (Malczewski and Rinner 2015). The criteria in MADA are defined by attributes, and the attributes can also be viewed as objectives (Malczewski 1999). In contrast, in MODA, the attributes serve as the means through which the objectives can be met. The set of

alternative are defined implicitly, but with explicit constraints (Malczewski 1999). This means that MODA works to find the best alternative based from the results produced within these constraints (Malczewski 1999).

There are numerous MADA decision rule methods that can be used in spatial decision problems: Weighted Linear Combination (WLC), Simple Additive Weighting (SAW), Analytic Hierarchy Process (AHP), and Ideal Point Methods (IPM) (Malczewski and Rinner 2015). The research presented in this paper focuses on multiattribute analysis (MADA), specifically Ideal Point Methods (IPM).

2.2. Ideal Point Methods

The ideal point is the hypothetical alternative that presents the most preferred weighted standardized value across the whole study area, after the criteria are combined. The negative ideal (nadir) point is the opposite of the ideal point, meaning the hypothetical alternative that presents the least preferred weighted standardized value across the whole study area (Malczweski 1999). Ideal Point Methods (IPM) are used to simultaneously determine the alternative that is the closest to the ideal point and the farthest away from the nadir point. The alternatives are calculated and ranked based on their geometrical distance from the ideal point and nadir point (Malczewski and Rinner 2015).

IPM can minimize some periodic difficulties related to correlations between different criteria, making it an often preferred approach when correlations exist between criteria (Malczewski 1999). This can be significant for spatial decision problems, which often include interdependent correlations (Malczewski 1999).

IPM has two primary techniques: Compromise Programming (CP) and Technique for Order Performance by Similarity to Ideal Solution (TOPSIS). TOPSIS is one of the most widely used IPM techniques (Malczewski 1999) and for the purposes of this study it will be used to assess earthquake vulnerability in the SFV. The technique was developed by Hwang and Yoon (1981).

2.2.1. Global GIS-MCDA Methods vs. Local GIS-MCDA Methods

GIS-based MCDA methods, such as TOPSIS, were developed as global approaches. This means that they do not take into consideration that the elements of GIS-based MCDA, such as weights and standardization, do not change over geographical space (Malczewski 2011). These methods assume spatial homogeneity within the study area for criteria weights and standardized values. For example, the TOPSIS technique assigns the same criterion weight to every decision alternative to each criterion. Therefore, global GIS-based MCDA methods do not take into account that spatial heterogeneity may exist due to various factors, such as social, economic, and environmental variances (Malczewski 2011).

Another disadvantage of Global GIS-MCDA methods is the way in which weights are assigned to criteria. In these methods, the decision maker is the one who decides the relative weights; therefore, the assignment of weights is subjective based on the decision maker's opinions and knowledge of the spatial decision problem (Boroushaki 2017). Based on reviews and surveys of method procedures, due to the subjective nature of subjective weighting methods, there is no way to overcome this advantage (Boroushaki 2017).

In order to overcome this disadvantage, weights can be estimated based on a normative theory, which is the range sensitivity principle (Malczewski 2011). In the range sensitivity principle, criterion weights are assigned to criterion values in large part based on the range of

values of the criterion (Malczewski 2011). This principle suggests that criterion with greater ranges of values should be assigned higher weights (Malczewski 2011). Based on this principle, local GIS-based MCDA models, such as Local WLC (Malczewski 2011) and Local TOPSIS (Qin 2013) were developed.

Due to the fact that local factors can influence the criteria values over geographical space, it is necessary to calculate the GIS-based MCDA steps considering local factors (Malczewski 2011). The local area is defined by the concept of neighborhoods; therefore the neighborhoods must be defined. The specific ways to define the size of the neighborhoods will be explained under Local TOPSIS in section 2.2.3.1.

2.2.2. Global TOPSIS

As previously mentioned, TOPSIS assigns overall scores to the alternatives based on their geometrical distance from the ideal and nadir point. It helps to find the ideal solution for the decision problem, which is the alternative that is simultaneously closest to hypothetical ideal point and farthest from the nadir point (see section 2.2).

2.2.2.1. Standardization

Global GIS-based MCDA methods assume spatial homogeneity and therefore standardization and criterion weights calculations are performed based on the whole study area (see section 2.2.1). The standardization method for Global TOPSIS will be performed using score range method. The formulas for standardizing criteria using score range method can be seen in section 2.1.1.

2.2.2.2. Criterion Weights

In global GIS-MCDA methods, same weight is assigned to all alternatives in a given criterion (see section 2.2.1). In this study global weights will be determined using the Pairwise Comparison method. The procedure of which the decision maker assigns weights to the criteria is explained in section 2.1.3.

2.2.2.3. Decision Rule

The geometrical distance between the ideal and nadir points and each alternative are also known as similarity to ideal point and similarity to nadir point, respectively. They can be calculated based on the following formulas:

$$s_i = \sqrt{\sum_{k=1}^{n} \left(w_k (v_k^* - v_{ik}) \right)^2} \tag{2.9}$$

$$d_i = \sqrt{\sum_{k=1}^{n} \left(w_k (v_{ik} - v_{k*}) \right)^2} \tag{2.10}$$

$$f_i = \frac{d_i}{s_i + d_i} \tag{2.11}$$

where s_i is the weighted distance (similarity) between the local ideal point and *i*-th alternative; d_i is the weighted distance (separation measure)s between the nadir point and *i*-th alternative; w_k is the global weight; v_k^* and v_{k*} are the maximum and minimum standardized values of the *k*-th criterion for the *i*-th alternative respectively; f_i is the relative closeness to the local ideal point for the *i*-th alternative.

2.2.3. Local TOPSIS

The concepts of spatial heterogeneity and range sensitivity principle play a central role in the local form of TOPSIS. Spatial heterogeneity can be reflected by neighborhoods, while the range sensitivity principle is taken into account the using local range as a function when standardizing the criteria and calculating local weights.

2.2.3.1. Neighborhood Definition

There are three main ways to define a neighborhood. One way is to divide the study area based on functional units, such as urban neighborhoods, land use zones, and geologic types (Malczewski 2011). The second way is by non-overlapping neighborhoods (blocks), meaning that neighborhoods are identified as fixed areas of equal sizes, and these areas stay the same throughout the calculations. The third way that a neighborhood can be defined is by the concept of moving windows. In this method, a focal point is identified as the center of the neighborhood, and the rest of the neighborhood is then defined proportionally around that point. Therefore, the neighborhood moves based on where the focal point is, resulting in overlapping neighborhoods (Malczewski 2011).

There are also different ways to define the shape and size of the neighborhood. The size of the neighborhood can either be fixed or floating, depending on the type of GIS data used. In GIS raster data, fixed neighborhood sizes are used due to the cells being the same shape and size. In GIS vector data, the neighborhood size is floating due to the variance in the sizes of the polygons (Qin 2013). Additionally, there two methods which can determine which cells or polygons will be included in the neighborhood thereby determining the size of the neighborhood: the adjacency measure and the distance-based measure. Adjacency measure considers two units or cells as

neighbors if they share a boundary. There are two main types to determine exactly if a unit is included or excluded from a neighborhood: Rook's case and Queen's case. In Rook's case, if two cells share two or more points, they are considered neighbors. In Queen's case, cells are considered neighbors if they share one or more points. Therefore, in Queen's case, a neighborhood includes all the cells that surround the focal point (Malczewski 2011). The adjacency method is a better fit for raster data (Malczewski 2011). In the distance-based method, a fixed distance radius around the focal point (cell or polygon) is determined. If the centroid of the adjacent cells falls within this radius, then the cells are included in the neighborhood (Malczewski 2011).

The use of Local TOPSIS in a GIS-based MCDA should be based on the type of criteria involved. If a criterion is made up of values that cover a large area in a continuous manner, the use of such a criterion would not be effective. This is due to local range being used as the denominator when standardizing the criteria. In a case of a criterion that consists of large areas of the same value continuously, a significant amount of neighborhoods would consist of the same values. The result would be that these values would be defined as null because it is impossible to divide by zero. Null values are omitted when aggregating the data through a decision rule method, and therefore large portions of a study area can be left without results, which make a study non efficient.

2.2.3.2. Local Range

In order to assign criterion weights, the range of values of each criterion must first be determined, as per the range sensitivity principle, which indicates that indicates that criterion values with greater ranges should be assigned higher criterion weights (Malczewski 2011). Malczewski (2011) defines local range formula as follows:

$$r_k^q = max_k^q\{a_{ik}\} - min_k^q\{a_{ik}\} \quad (2.12)$$

where $max_k^q\{a_{ik}\}$ is the maximum criterion value for the *k*-th criterion in the *q*-th neighborhood and $min_k^q\{a_{ik}\}$ is the minimum criterion value for the *k*-th criterion in the *q*-th neighborhood.

2.2.3.3. Local Standardization

Value scaling or standardization is an essential element in in GIS-based MCDA process, as it transforms the different criteria values into the same unit of measurement (see section 2.1.1). Malczewski (2011) defines the local standardization formula as follows:

$$v_k^q = \frac{a_{ik} - min_k^q\{a_{ik}\}}{r_k^q} \quad (2.13)$$

or

$$v_k^q = \frac{max_k^q\{a_{ik}\} - a_{ik}}{r_k^q} \quad (2.14)$$

where $min_k^q\{a_{ik}\}$ and $max_k^q\{a_{ik}\}$ relate to the minimum and maximum criterion value for the *k*-th criterion for the *i*-th alternative in the *q*-th neighborhood respectively; r_k^q is the local range that can be calculated using Equation 1. v_k^q represents the local standardized value that ranges from 0 to 1. Equation 3.13 is used to standardize maximization criteria, while Equation 2.14 is used to standardize minimization criteria.

2.2.3.4. Local Criterion Weights

Local weighting is based on the range sensitivity principle. Once global weights have been determined, local weights can be determined as a function of the global weight, global and local

ranges (Malczewski 2011). Malczewski (2011) defines localizing criterion weights by the following formula:

$$w_k^q = \frac{\frac{w_k r_k^q}{r_k}}{\sum_{k=1}^{n} \frac{w_k}{r_k}} \quad 0 \le w_k^q \le 1 \; and \; \sum_{k=1}^{n} w_k^q = 1 \tag{2.15}$$

the local weight, w_k^q, is determined by the global weight (w_k), global range (r_k), and local range (r_k^q). Global range and global weight are consistent across the whole study area, while local weights depend on the local range in each neighborhood q. Weights can only have a value between 0 and 1 and the sum of all weights has to be equal to 1.

2.2.3.5. Decision Rule

TOPSIS aims to find the alternative, which is the closest to the ideal point and the farthest from the negative point. In Local TOPSIS, the calculations of the weighted standardized criteria values are based on the local ideal and nadir points in the defined neighborhood (see section 2.3.5.5). Local TOPSIS can be formulated as follows:

$$s^q = \sqrt{\sum_{k=1}^{n} \left(w_k^q \frac{v_k^q - v(a_{ik})_*^q}{v(a_{ik})^{q*} - v(a_{ik})_*^q} \right)^2} \tag{2.16}$$

$$d^q = \sqrt{\sum_{k=1}^{n} \left(w_k^q \frac{v_k^q - v(a_{ik})_*^q}{v(a_{ik})^{q*} - v(a_{ik})_*^q} \right)^2} \tag{2.17}$$

$$f^q = \frac{d^q}{s^q + d^q} \tag{2.18}$$

where s^q is the weighted distance (similarity to ideal point) between the local ideal point (LIP) and *i*-th alternative within the *q*-th neighborhood; d^q is the weighted distance (similarity to nadir point) between the local nadir point (LNP) and *i*-th alternative within the *q*-th neighborhood; w_k^q is the local weight; $v(a_{ik})^{q*}$ and $v(a_{ik})_*^q$ are the minimum and maximum standardized values of the *k*-th criterion for the *i*-th alternative within the *q*-th neighborhood, respectively; f^q is the relative closeness to the LIP for the *i*-th alternative.

2.3. Risk and vulnerability

Vulnerability represents the level of risk to natural hazards and constitutes the potential loss predictor during a natural hazard (Armas 2012). There is great variability in the impacts of environmental hazards, both in the size and type of impact that they can have. Therefore, it is important to have interdisciplinary teams of professionals managing assessment of risk and vulnerability. Due to the range of potential impact of hazards, such as physical, social, political, and economical, risk reduction efforts should encompass all potential impacts (Servi 2004). It is also important to mention that vulnerability cannot be measured directly, but can be estimated indirectly based on a number of criteria related level of damage caused by a natural hazard (Armas 2012).

In order to understand the concept of risk, it is necessary to understand what a hazard is. A hazard is a phenomenon that can cause damage to people or property. The magnitude of a hazard is the level of damage caused by the hazard. As previously mentioned, vulnerability is a complex term that encompasses a number of different factors that are susceptible to harm, while risk is the level of potential losses due to a hazardous event (Servi 2004). Risk can be thought of as the probability of hazards happening and the degree of vulnerability (risk = hazard * vulnerability)

(UN 1991). Therefore, two towns located in an active seismic zone with similar physical settings will not be equal in risk if they differ in the vulnerabilities to an earthquake. Differences in vulnerability would mean differences in the capacity to cope and tolerate damage caused by an earthquake (Rashed and Weeks 2003). Capacity is the combination of all resources available within a community, which can reduce the effects of the disaster. In the process of mitigation, raising the capacity of an urban system to respond to natural hazards would reduce the vulnerability to the hazard (Armas 2012).

2.4. Urban vulnerability to earthquakes

At the end of the second millennium, half of the global population lived in cities and It is expected that as many as 70% of people will live in cities by 2050 (Armas 2012). This is a concerning pattern due to the fact that 40% of the world's major urban centers are located within 200 km of a tectonic plate boundary or of a region that experienced an earthquake in the past (Ploeger, Atkinson, and Samson 2009).

Owing to the inability to predict the location, occurrence and magnitude of an earthquake, it is necessary to create mitigation plans that are based on past earthquake events and vulnerability assessments of specific cities or regions. Properly planned mitigation strategies can prevent human loss and also lessen the effects of an earthquake (Levi et al. 2014). Mitigation plans can focus on areas with higher vulnerability to earthquakes in order to reduce the amount of damage and implement preventative measures, such as updating building codes (Walker et al. 2014). Vulnerability assessment can also help decision makers decide how to allocate limited resources in the case of an emergency (Levi et al. 2014). Owing to the implementation of mitigation plans in a manner to enforce strict buildings codes, there has been a reduction of physical, social and

economic losses from earthquakes, mostly in developed countries (Ploeger, Atkinson, and Samson 2009).

Vulnerability assessment of urban environments in regard to natural hazards and earthquakes in particular has become a major research topic for the geologists and engineers in the academic world in the last two decades (Uitto 1998, Menoni et al. 2002, Rashed and Weeks 2003, Crowley, Pinto, and Bommer 2004). In the last decade, there has been a shift in the literature towards more local analyses of vulnerability (Ploeger, Atkinson, and Samson 2009, Moffatt and Cova 2010, Martins, Silva, and Cabral 2012, Armas 2012, Walker at al. 2014, Panahi, Rezaie, and Meshkani 2014). These studies focus on smaller areas rather than larger areas in order to be able to produce more accurate predictions of vulnerability on a smaller scale.

In the next sections, the criteria that will be used in this study will be described with regard to their effect on damage caused by earthquakes.

2.4.1. Distance to Epicenter

In seismology, the epicenter relates to the point on Earth's surface that is directly above the hypocenter (the subsurface point where the fault ruptures). In an earthquake, seismic waves are released in a spherical shape from the hypocenter. As the waves travel away from the hypocenter, the size of the sphere grows, therefore the energy of the wave is spread out over a larger area. As the energy decreases, the impact on Earth's surface also decreases (Lowrie 2007). The closer an urban area is to an earthquake's epicenter, the higher the risk level of sustaining damage when compared to areas that are farther away from the epicenter (Lowrie 2007).

2.4.2. Average Shear Wave Velocity

Shear wave velocity relates to the speed that a shear wave or S-wave follows primary waves or P-waves. Shear waves travel with oscillations perpendicular to the direction of the wave's motion (Lowrie 2007).

Shear wave velocity can give an indication of whether the ground shaking at a specific location may be higher or lower. The velocity of the shear waves varies depending on the density and the material through which they pass. In general, the average shear wave velocity is heavily dependent on the soil or rock type. Seismic waves can travel through hard igneous rock to soft, loose sand. Waves generally slow in softer soils, and as a result they compress with the wave amplitude increasing, thereby causing more intense ground shakes at these sites. Soil softness is determined by mineral grain size. Larger grain size means softer soil because large granules shift around easily and do not interlock. Sand has a larger grain size than silt and silt has a larger grain size than clay.

Soil stiffness also depends on the percent moisture present in the soil. Higher moisture values can cause soil collapse owing to loss of soil structure strength. This in turn potentially leads to greater damage to buildings. Thus, ground covered with sand that contains higher levels of moisture produces more ground shake than ground covered with clay or silt. Sometimes, ground is composed of more than one soil type, as in loam. In this case the ground shake is determined by the percentage of each soil type in the mixture (U.S. Geological Survey n.d. a).

In contrast to soil, ground made of hard rock, such as granite, and not covered with soil, generally has the least intensity of ground shaking during an earthquake. This is because hard rock speeds up wave travel and forms smaller waves, producing less ground shake than soil. In an area covered with soil, the presence of bedrock under the soil dampens the oscillation of

waves, resulting in less ground movement. Areas with bedrock have a shaking intensity at least three times less than those with only softer soils. As a result, when the waves move from rock to soft soil, they get bigger as they need to carry the same amount of energy, thus creating stronger shaking ground shaking (FEMA n.d., U.S. Geological Survey n.d. a).

2.4.3. Damage Caused by Structures

Two important variables affecting earthquake damage are intensity of ground shaking and the quality of the engineering of structures in the region. Generally, the bigger, closer, and shallower the ground shake, the stronger the earthquake (IRIS and University of Portland n.d.). However, there have been large magnitude earthquakes with little damage because they were far from populated areas, or because the buildings were built to withstand large earthquakes. On the other hand, there have been moderate earthquakes that caused significant damage either because buildings were not constructed according to earthquake suitable codes or construction materials cannot withstand ground shaking (IRIS and University of Portland n.d.).

The main factor for casualties in an earthquake event is actually not the magnitude of ground shake, but in fact how man-made structures withstand an earthquake. For instance, a city in a developing country could suffer higher number of casualties from a lower magnitude earthquake compared to a city in a developed country that would be affected from a higher magnitude earthquake. The reason is that in developing countries, houses and buildings are often built from mud, clay or wood, or may be built with sub-standard materials, whereas in developed countries buildings may have to conform to rigorous standards for frame construction and wall and window structures.

In addition, since the twentieth century, the interdisciplinary branch of earthquake engineering has been developed in order to make structures more resistant to earthquakes. In the United States, the Federal Emergency Management Agency (FEMA) is the governmental body, which is responsible for publishing recommended seismic provisions for buildings. These provisions are also called seismic codes, and structures such as buildings, roads and bridges are built in accordance to them. Generally, older buildings have higher risk of sustaining damage caused by an earthquake than newly constructed buildings. The reason is that seismic codes are issued every few years based on newly discovered technologies that can assist in designing earthquake resistant structures (FEMA 2017).

2.4.4. Slope

Another factor that can impact vulnerability to earthquakes is slope instability. When slope instability is greater, this can often lead to landslides, which have historically been the cause of significant damage and death from earthquakes (Moore et al. 2012). Slope stability is dependent on several factors, including soil structure and composition, geometry, and groundwater conditions (Tucker, Erdik, and Hwang 1993). Slope instability can increase over time from different types of events, but instability can also be caused by one triggering event, such as an earthquake (Nelson 2013). Though earthquakes can trigger the failure of the slope, the slope may already been weakened by other factors such as erosion, sedimentation, and human influences (Hack et al. 2007).

It is clear that earthquakes have a great effect on slope stability, however the science and calculations of exactly what the impact will be are difficult to measure due to the variety of factors and three-dimensional analysis required (Hack et al. 2007). Improving the ability to

estimate slope stability during an earthquake, and using this information in vulnerability analysis, is important in order to prevent the mass damage and casualties that can result from earthquake-induced landslides (Hack et al. 2007).

3. Data and Methodology

3.1. Study Area

The SFV is an urbanized area in Southern California and covers about 260 mi^2. Most of the SFV is within jurisdiction of the city of Los Angeles, although there are other incorporated cities that are located within in the SFV: Burbank and part of Glendale are located in the southeast corner of the SFV, Hidden Hills and Calabasas lie in the southwest corner of the SFV, San Fernando in the northeast of the SFV, and Universal City, which is an unincorporated area, in the southern part of the SFV.

The SFV is bordered by the San Gabriel Mountains to the north and northeast, Santa Susana Mountains to the northwest, Simi Hills to the west, Santa Monica Mountains and Chalk Hills to the south, and Verdugo Mountains to the east (Encyclopedia Britannica 2011). These mountain ranges are part of the Transverse Ranges, that trend east-west relative to the orientation of the bulk of mountain ranges in California and are populated with dominantly thrust and reverse fault systems. In addition, the San Andreas fault, though located some 30 km north and northeast of the SFV and capable of producing event in excess of 8Mw, adds a complex, geologic structure characterized by strike-slip motion (DeCourten 2006). Southern California experiences about 10,000 earthquakes annually, although most of them are too small to be felt (U.S. Geological Survey n.d. a). This research focuses on the Sierra Madre fault zone and in particular the Santa Susana fault.

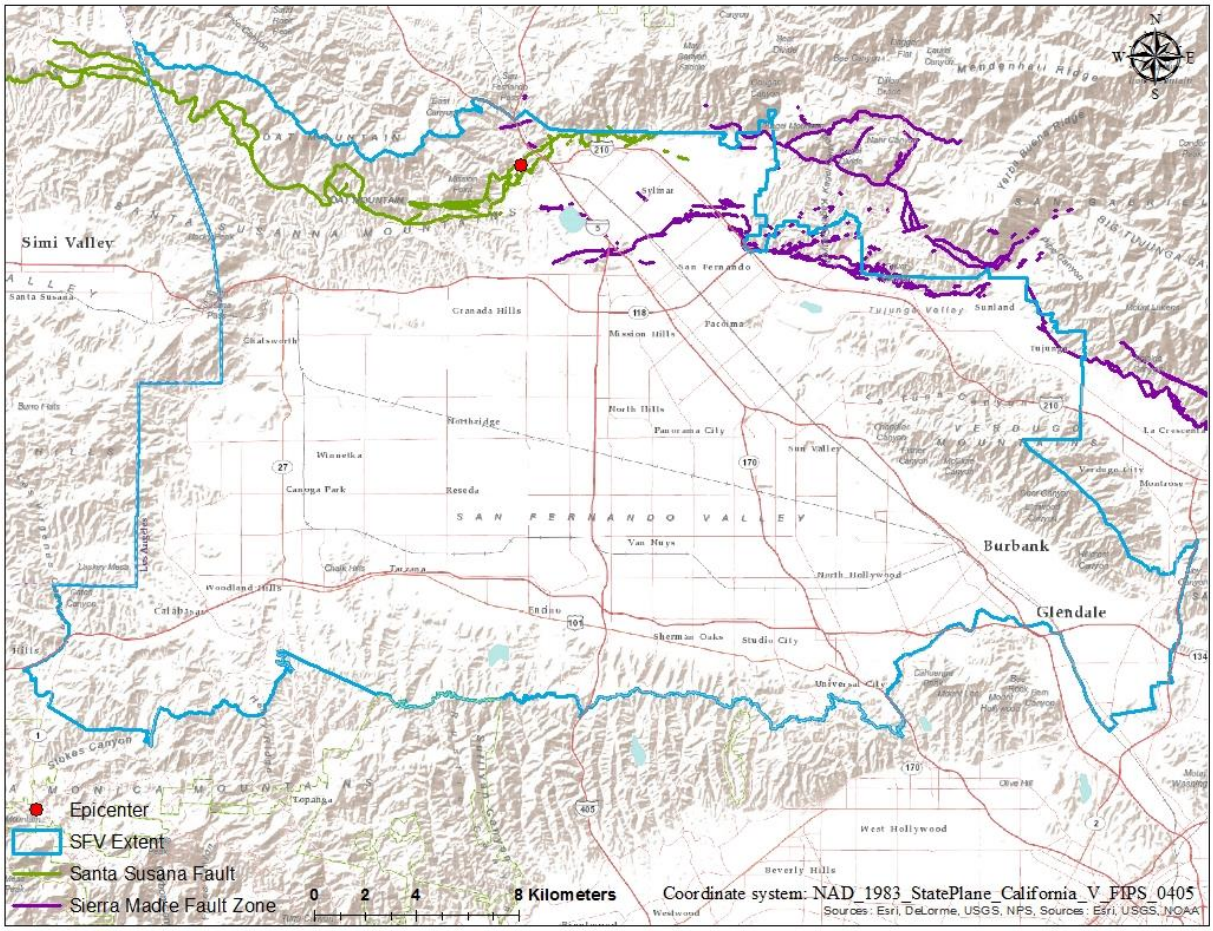

Figure 3.1. Extent of the SFV (light blue**)** in relation to the epicenter (red dot), which was placed on Santa Susana Fault (green), which is part of the Sierra Madre Fault Zone (purple).

3.1.1. Background in Seismic Activity

The Sierra Madre fault zone includes the San Fernando, the Santa Susana, and the Sierra Madre faults.

Capable of producing a 7.0-7.3 Mw event (Southern California Earthquake Data Center 2013 a, Southern California Earthquake Data Center 2013 b), the Santa Susana fault is located on the northwest edge of the SFV, and stretches westwards some 28 km into Ventura County. As is the case with most faults, the Santa Susana fault does not have a flat surface, and there are ramps that connect the different flat segments of the fault (Twiss and Moores 1992). The Santa Susana

fault has two ramps. The smaller ramp, the Gillibrand Canyon ramp, impacted the distribution of aftershocks of the 1994 Northridge earthquake. The larger ramp, the San Fernando or Chatsworth ramp, is where the main shock and many aftershocks of the Sylmar earthquake in 1971 took place. The 1893 Pico Canyon earthquake may have also taken place on the Santa Susana fault. The fault has a dip-slip rate of 2.1 to 9.8 mm per year (Dolan et al. 2001).

The Santa Susana fault grades eastwards into the Sierra Madre fault, which is exposed for 75 km at the base of the San Gabriel Mountains. The two faults differ from each other in that the Santa Susana fault is located on the southern slopes of the Santa Susana Mountains, and the Sierra Madre fault is located at the base of the mountains. The Sierra Madre fault is estimated to have a slip rate of at least .6 mm per year, which is believed to have been caused by two earthquakes ranging in magnitude from 7.2Mw to 7.6Mw. Some of the aftershocks of the 1971 Sylmar earthquake were produced by the Sierra Madre fault (Dolan et al. 2001).

The San Fernando fault was the result of a 15 km rupture caused by the 1971 Sylmar earthquake south of the Sierra Madre fault. The 1971 Sylmar (6.6Mw) resulted in 64 deaths and over 2,500 injured. There was also extensive damage to buildings and city infrastructure (Dolan et al. 2001).

There are also a number of south dipping reverse faults in the area, such as the Northridge blind thrust fault (no surface break). This fault was responsible for the 1994 Northridge Earthquake, which was the earthquake that caused the most damage in United States history. The earthquake occurred on a fault that was unmapped and was plunged beneath the Santa Susana Mountains and the Western SFV. This fault is the eastern continuation of the Oak Ridge fault. The Northridge earthquake (6.7Mw) resulted in a death toll estimated at around 60 people, and

damage was caused for up to 85 miles (125 km), including damage to buildings and freeways, along with fires and disrupted water and natural gas systems (Dolan et al. 2001).

3.2. Data

Four criteria will be used for the vulnerability assessment process: 1) proximity to epicenter, 2) structure year built, 3) average shear wave velocity, and 4) slope (Table 3.1).

The data for this research was obtained from a few different sources: structure year built data was downloaded as a feature class from Los Angeles County GIS Data Portal (Los Angeles County GIS Data Portal 2016). Average shear wave velocity, Vs30, was obtained from USGS Earthquake Hazards Program (U.S. Geological Survey n.d. b), and Digital Elevation Model (DEM) data for slope calculation was downloaded from USGS' National Elevation Dataset (U.S. Geological Survey 2017). In addition, Census the block groups layer was obtained from Los Angeles County GIS Data Portal (Los Angeles County GIS Data Portal 2016).

3.3. Methodology

After the criteria data was downloaded, each criterion had to be cleaned and organized. The analysis and its relevant steps were executed in ArcGIS' ArcMap software.

Owing to the fact that the SFV area includes a number of different cities, the extent of the SFV area for this research was defined visually using ArcMap. The census block group layer was edited manually in order to be compatible with the defined extent of the SFV. Before converting to raster datasets, all relevant criteria feature classes were projected onto California State Plane Zone 5, which is part of the North American Datum 1983. This is the proper projection for Los Angeles County (State of California – Department of Conservation 2017). In addition, the census

block groups feature class was converted from polygon to raster, and output raster datasets for all criteria were produced based on the area of the census block groups.

The next sub-sections will explain how the different criteria were edited and prepared in order for them to be ready to use in the MCDA process.

Table 3.1. Criteria used for assessing vulnerability of buildings to earthquake.

#	Name	Objective Direction	Studies that Used this Criteria to Assess Vulnerability to Earthquakes
1	Distance to Epicenter	MIN	Otani (2000), Hizbaron et al. (2011), Erden and Karaman (2012)
2	Slope	MAX	Panahi, Rezaie, and Meshkani (2014), Delavar, Moradi and Moshiri (2015), Sheikhian, Delavar and Stein (2015)
3	Structure Year Built	MIN	Cochrane and Schaad (1992), Ahmed, Jahan and Alam (2014), Panahi, Rezaie, and Meshkani (2014), Delavar, Moradi and Moshiri (2015)
4	Average Shear Wave Velocity	MIN	Anbazhagan et al. (2010), Karimzadeh et al. (2014), Karapetrou, Fotopoulou and Pitilakis (2015)

3.3.1. Distance to Epicenter

The epicenter point was placed on the portion of the Santa Susana Fault, which is located in the SFV near Granada Hills. The Sierra Madre Fault Zone, which contains the Santa Susana Fault, was responsible for a few of recent major earthquakes, such as the 1971 Sylmar earthquake. In addition, the Santa Susana fault has a high slip rate of 2.1 to 9.8 mm per year (see section 3.1.1). The raster created for this criterion holds values of the distance in meters to the epicenter for each cell (alternative) (Figure 3.2). This is a minimization criterion because areas closer to an earthquake epicenter are more vulnerable to higher physical damage than areas that are further away (see section 2.4.1).

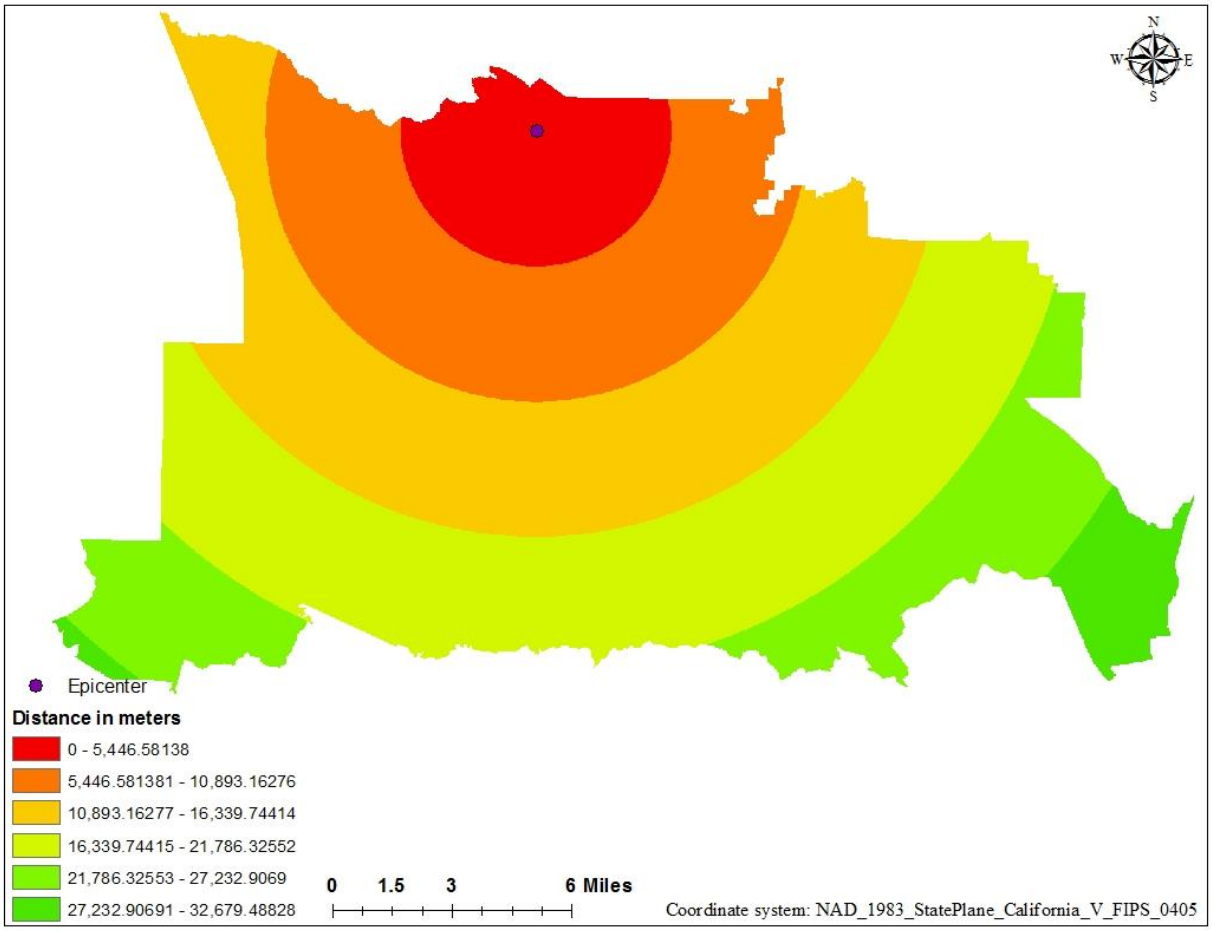

Figure 3.2. Distance to Epicenter criterion map.

3.3.2. Average Shear Wave Velocity

For average shear wave velocity data, Vs30 data was used. Vs30 is the average shear wave velocity in the top 30 meters of earth's surface (Brown, Diehl and Nigbor 2000). Average shear wave velocity (Vs30) was downloaded as a point layer, and converted to raster using Inverse Distance weighting interpolation (IDW). IDW calculates the value of a point based on the values of the points close by, based on the assumption that things that are close to each other have more similar values (Lu and Wong 2008). IDW assumes that the value of an un-sampled point is equal to the weighted average of other known points in the same neighborhood (Lu and Wong 2008). In this study, the neighborhood was defined by the twelve closest points to the un-sampled point.

This is a minimization criterion because shear waves create more damage as they move slower (see section 2.4.2).

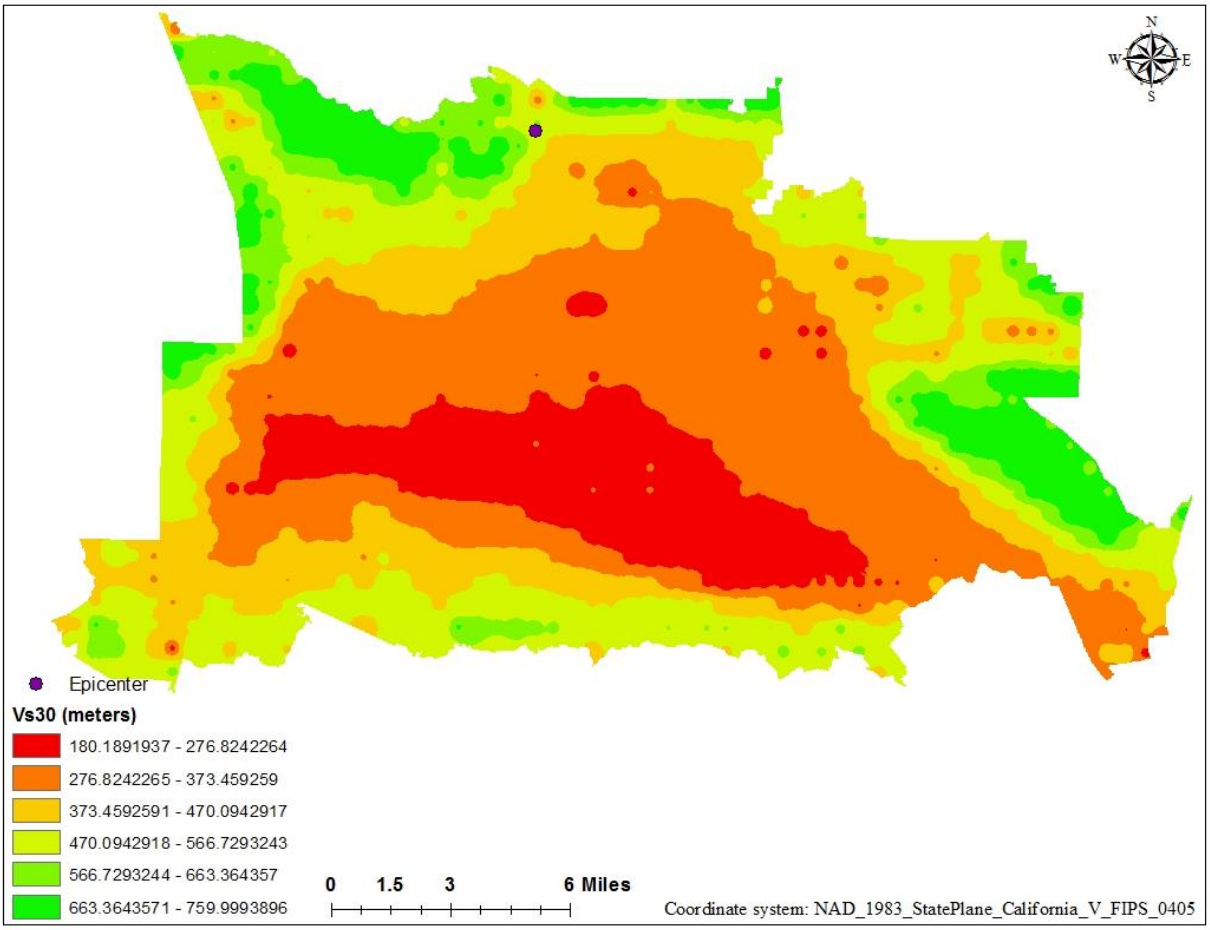

Figure 3.3. Average Shear Wave Velocity criterion raster.

3.3.3. Structure Year Built

Effective year built was selected to represent the structure year built criterion. Features without a year built value were deleted. Effective year built is one of the fields in the building footprints feature class. Effective year built is the adjusted year built of the building taking into account any major renovations or retrofitting. A total of 532,307 buildings with effective year built value were included in the criterion. To create the raster for this criterion, first the building

footprints that are located in the SFV were selected. Then, these footprints were converted from polygon to raster. In contrast to the other criteria, this criterion does not cover the whole area of the SFV determined for this research, as, naturally, buildings do not cover the whole study area. This is a minimization criterion because older buildings were not built according to updated seismic codes and are therefore at greater risk (see section 2.4.3).

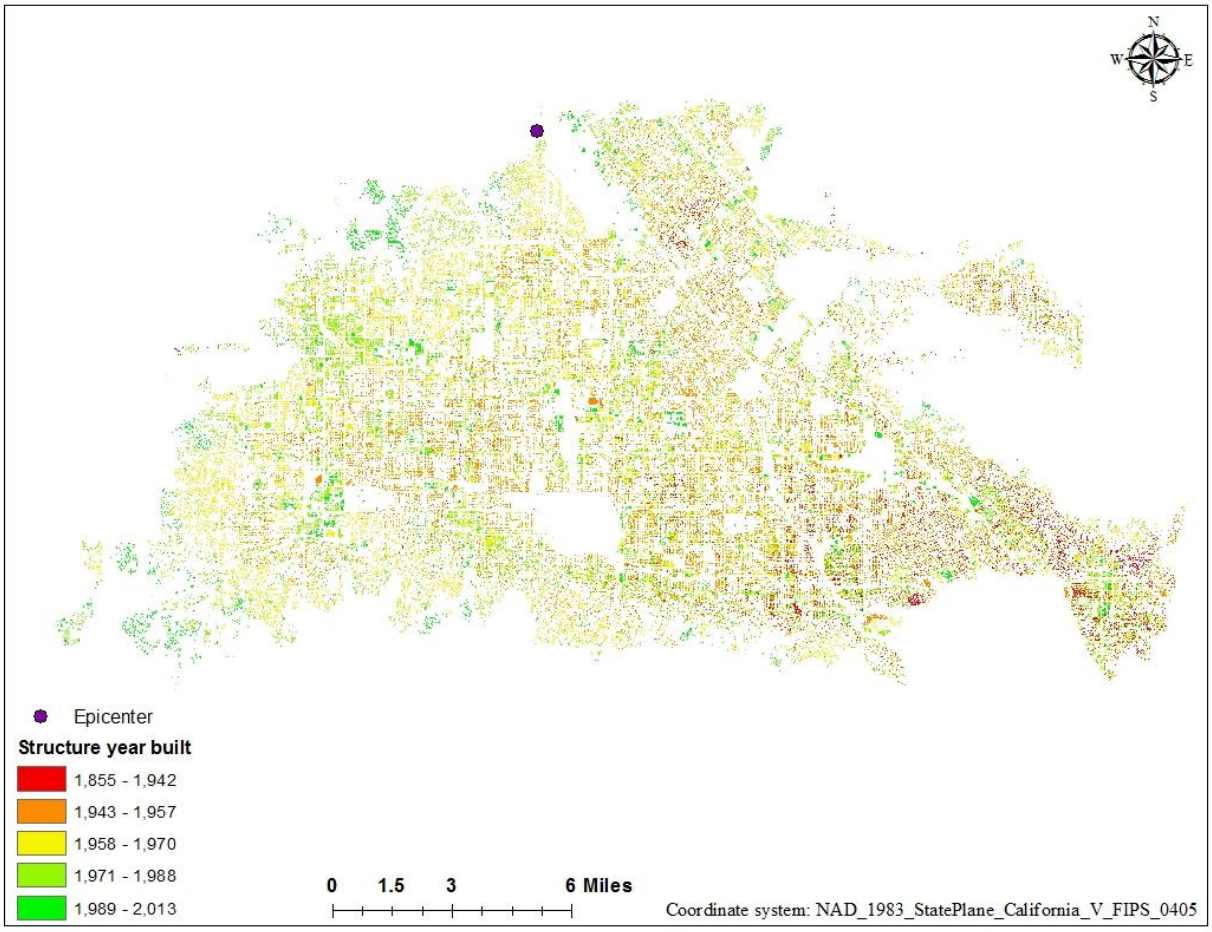

Figure 3.4. Structure Year Built criterion raster.

3.3.4. Slope

Slope was calculated based on the Digital Elevation Model (DEM). DEM is a digital model of earth's surface, created from elevation data. DEM data was downloaded for the area of LA County as a 1/3 arc second (approximately spatial resolution of 10 meters) raster dataset. Then,

the slope raster was produced as a percentage rise based on the DEM raster. This is a maximization criterion due to the fact that an area with high percent rise of slope is more vulnerable to landslides than an area with low percent rise of slope (see section 2.4.4).

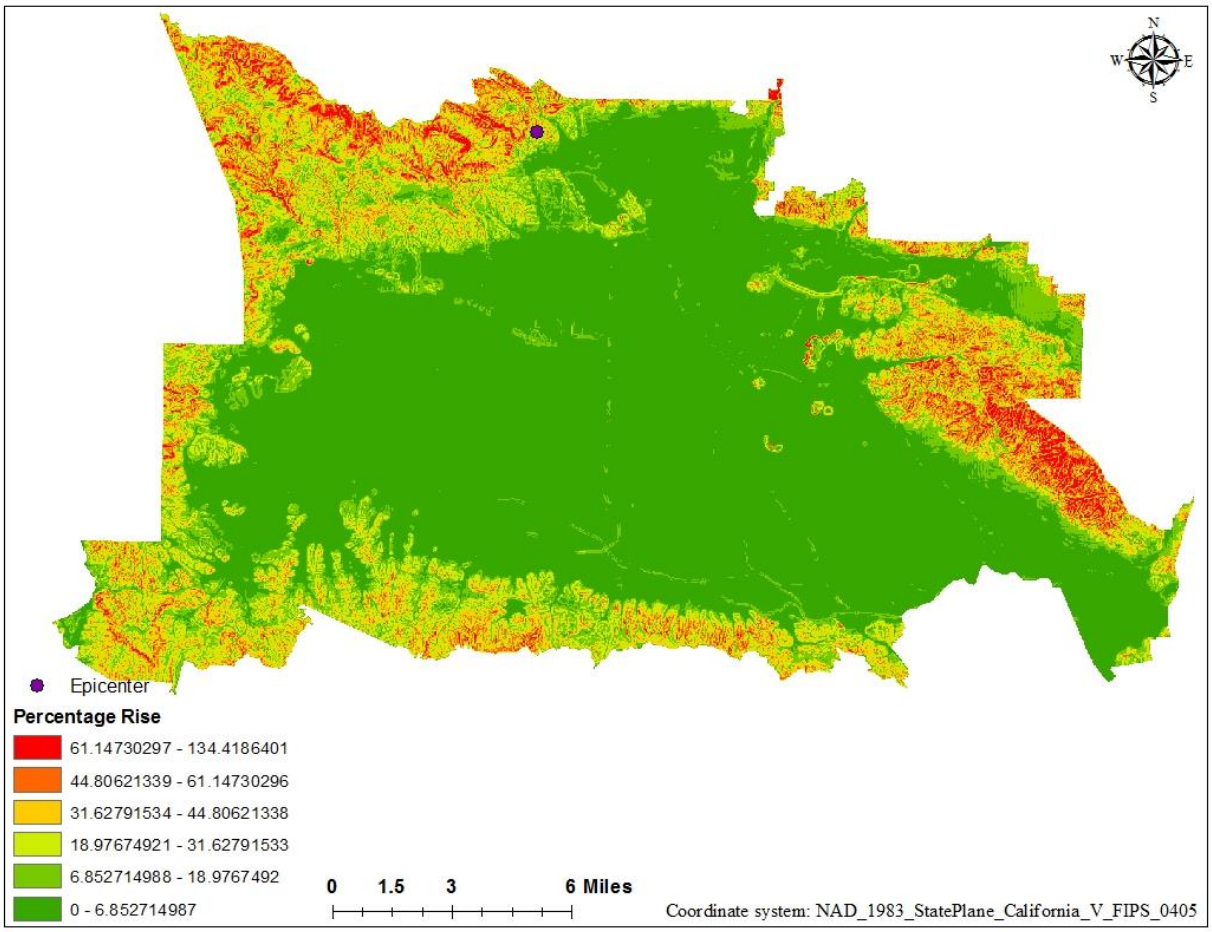

Figure 3.5. Slope criterion raster.

3.3.5. GIS-based MCDA Methods

The next sub-sections will describe the process of MCDA and its relevant steps. The MCDA process was calculated and performed using ArcGIS Model Builder. A single model containing all steps was created for Local and Global TOPSIS, respectively. Parts of the models will be presented in the next sub-sections for each relevant step.

3.3.5.1. Global TOPSIS

In this study, the standardization process was performed as part of the Global TOPSIS model that was created in ArcGIS Model Builder. An example of global standardization for structure year built, as used in the model can be seen in Figure 3.12. Year_Built represents the raw data criterion raster. The maximum and minimum values (YB_Max & YB_Min) of this criterion were obtained. Standardization was performed using the score range method. As structure year built is a minimization criterion, score range formula for minimization criteria was used (Equation 2.4).

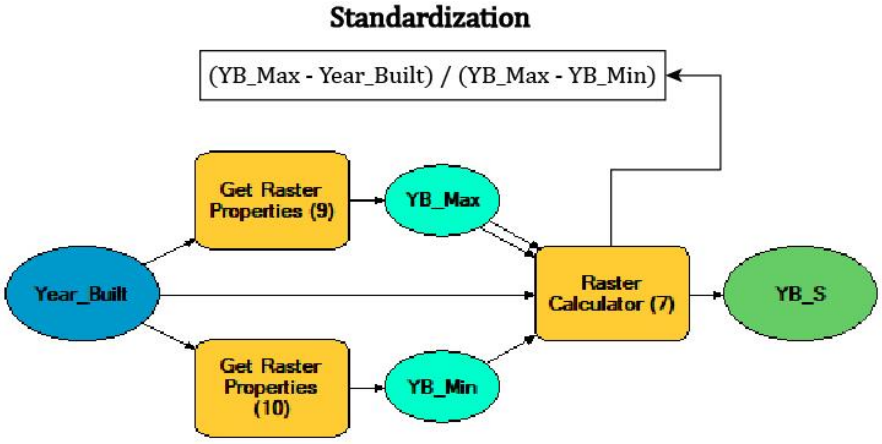

Figure 3.6. Standardization for structure year built (part of the Global TOPSIS model).

The next step was calculation of criterion weights. In this study, global weights were assigned to the criteria using the Pairwise Comparison technique (see section 2.1.2). The Pairwise Comparison of the criteria was done with advisement from Dr. Amalie Orme.

Table 3.2. Pairwise comparisons matrix.

		C1	*C2*	*C3*	*C4*
C1	*Proximity to epicenter*	1	2	4	8
C2	Slope	0.500	1	3	7
C3	*Construction year of building*	0.250	0.333	1	5
C4	*Average shear wave velocity*	0.125	0.143	0.200	1
	Sum	***1.875***	***3.476***	***8.200***	***21.000***

Table 3.3. Criterion weights matrix.

		C1	*C2*	*C3*	*C4*	**Weights**
C1	*Proximity to epicenter*	0.533	0.575	0.488	0.381	**0.494**
C2	Slope	0.267	0.288	0.366	0.333	**0.313**
C3	*Construction year of building*	0.133	0.096	0.122	0.238	**0.147**
C4	*Average shear wave velocity*	0.067	0.041	0.024	0.048	**0.045**
	Sum	***1.000***	***1.000***	***1.000***	***1.000***	***1.000***

Table 3.4. Consistency vectors matrix.

			Sum	**Consistency vector**
C1	*Proximity to epicenter*	0.494*1+0.313*2+0.147*4+0.045*8	2.07	**4.19**
C2	Slope	0.494*0.5+0.313*1+0.147*3+0.045*7	1.32	**4.20**
C3	*Construction year of building*	0.494*0.25+0.313*0.333+0.147*1+0.045*5	0.60	**4.07**
C4	*Average shear wave velocity*	0.494*0.125+0.313*0.143+0.147*0.2+0.045*1	0.18	**4.03**

Table 3.5. Consistency ratio matrix.

lambda=	4.12
CI =	0.04
CR=	**0.05**

The pairwise comparison matrix (Table 3.2), where each set of criteria were compared and ranked, was created using the pairwise comparison scale (Figure 2.1). The rankings were normalized by dividing the relevant ranking by the sum of its column (Equation 2.5). Then, weights were calculated according to the sum of values across each criterion, divided by the number of criteria (Equation 2.6) (Table 3.3). Consistency vectors were calculated according to the sum of ratings, multiplied by weights across each criterion, divided by the weight of the criterion (Table 3.4). Lambda represents the average of the consistency vectors. The consistency index was calculated by dividing the difference between the number of criteria and lambda by the number of criteria minus one (Equation 2.7) (Table 3.5). Lastly, the consistency ratio was calculated by dividing the consistency index by the random index (Equation 2.8). The random index is dependent on the number of criteria, which in this case are four. The random index value

for four criteria is 0.89 (Table 2.1). It is evident that the comparisons between the criteria are consistent as the consistency ratio is smaller than 0.10 (see section 2.1.2) (Table 3.5).

The next step was the calculation of similarity to ideal point (IP) and similarity to nadir point (NP). An example of similarities to IP and NP for structure year built, as used in the model, can be seen in Figure 3.7. The maximum and minimum values (YB_SMax & YB_SMin) were obtained from the standardized raster (YB_S). Weights were used in this model as parameters and were inserted manually for each criterion after clicking on the run model button. Similarity to IP was calculated based on Equation 2.9, where the weight (YB_Weight) was multiplied by the difference between the maximum value (YB_SMax) and the standardized values (YB_S) and then the result of these operations was squared. Similarity to NP was calculated based on Equation 2.10. For structure year built criterion, its weight (YB_Weight) was multiplied by the difference between the standardized value (YB_S) and the minimum value (YB_SMin). Then the result of these operations were squared.

The last step of the model is demonstrated in Figure 3.8. Aggregations of similarity to IP and of similarity to NP for all criteria were performed using square root sum. Then, Closeness to IP was calculated based on Equation 2.11. Similarity to NP (SqrtSum_SNP) was divided by the sum of similarity to NP and similarity to IP (SqrtSum_SIP).

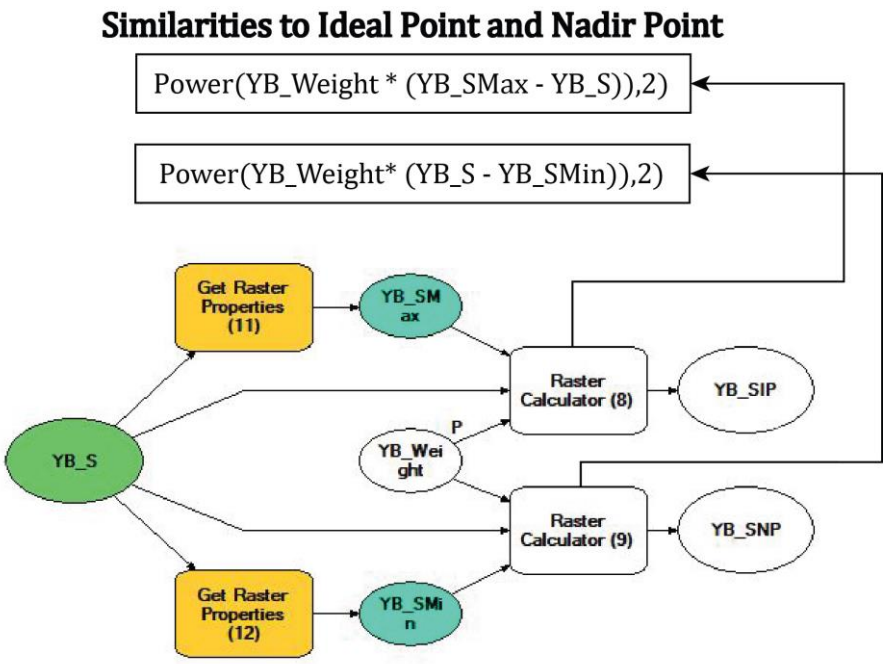

Figure 3.7. Calculation of similarity to IP and similarity to NP (part of the global TOPSIS model).

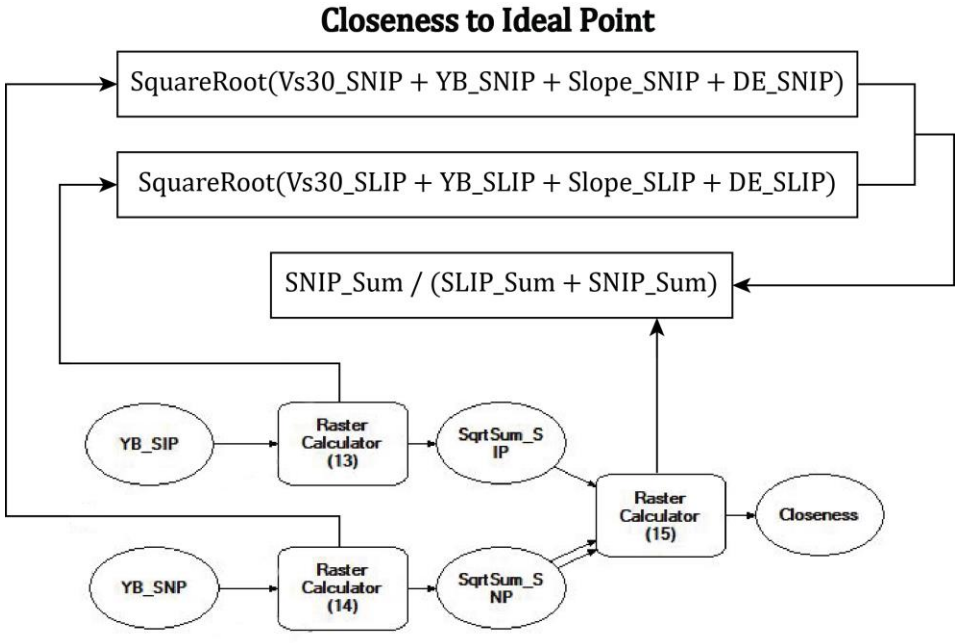

Figure 3.8. Aggregation of both similarity to IP and similarity to NP raster datasets and calculation of closeness to ideal point (part of the global TOPSIS model).

3.3.5.2. Local TOPSIS

This section will explain the steps of Local TOPSIS method. As previously mentioned in the literature review, neighborhoods that contain the same value in all of the cells produce null values in the Local TOPSIS process due to the fact that local range serves as the denominator when standardizing the values in Local TOPSIS. In neighborhoods with the same values in all cells, the range would be zero, and numbers cannot be divided by zero (see section 2.2.3.1). In this study, different size neighborhoods will be examined through the Local TOPSIS process in order to find the one that causes the least data loss. The following neighborhood sizes were tested: 3x3, 5x5, 7x7, 9x9 and 11x11. While it is important to prevent data loss by making the neighborhood size bigger, it is also important not to overlook other local factors when making the neighborhood size bigger. As a result, as the neighborhood size gets bigger, the Local TOPSIS method becomes more similar to the Global TOPSIS method, as less local factors are being considered. Therefore, it is important to find the neighborhood size that will cause the least amount of data loss while still maintaining a small neighborhood size.

In order to obtain the number of missing cells for each neighborhood size, the following steps were performed. First, cells that did not contain data were assigned the value of 1 and cells that contained data were assigned the value of 0. This procedure was performed over the closeness to ideal point raster datasets produced in the Local TOPSIS and Global TOPSIS models. Then, Local TOPSIS raster datasets (for each neighborhood size) produced in the previous step were compared with the Global TOPSIS raster produced in the previous step, one at a time. By adding the models' raster datasets, cells with the value of 1 are the missing cells in the relevant Local TOPSIS raster, as they only exist in the Global TOPSIS raster.

Table 3.6. Number of missing cells (value = 1) for 3x3 neighborhood size.

0	84,704
1	44,672

Table 3.7. Number of missing cells (value = 1) for 5x5 neighborhood size.

0	117,741
1	11,635

Table 3.8. Number of missing cells (value = 1) for 7x7 neighborhood size.

0	125,472
1	3,904

Table 3.9. Number of missing cells (value = 1) for 9x9 neighborhood size.

0	127,690
1	1,686

Table 3.10. Number of missing cells (value = 1) for 11x11 neighborhood size.

0	128,565
1	811

A value of 1 represents the missing cells compared to the Global TOPSIS closeness to IP. Based on these results, the neighborhood size of 9x9 cells was chosen to define the neighborhood size used in this study (Table 3.9). The reason is that use of 9x9 neighborhoods caused a relatively small amount of data loss compared to smaller sized neighborhoods, but also kept the neighborhood a relatively small size, which helped in maintaining the locality of the method.

After the neighborhood size was defined, Local Range could be calculated. In this study, Local Range was calculated as part of the Local TOPSIS model. Focal Statistics was used to calculate Local Range for neighborhoods of 9x9 cell size (Figure 3.9).

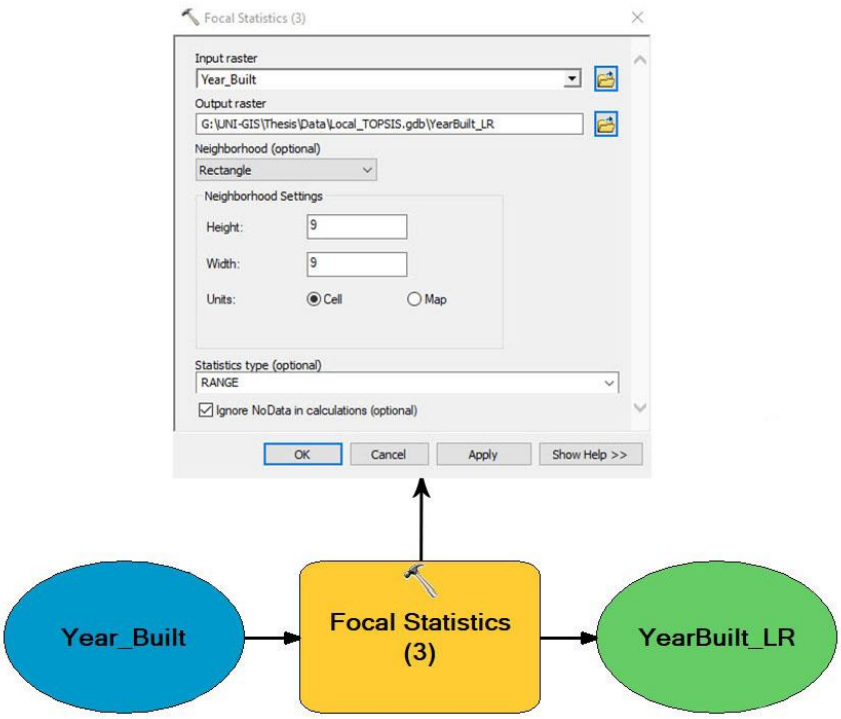

Figure 3.9. Calculation of Local Range for structure year built (part of the local TOPSIS model).

The next step was standardizing the raw values. Standardization is an essential step in GIS-MCDA analysis and is used to convert the different criteria scales into the same scale. In Local TOPSIS, the local value was calculated based on the values of the alternatives within its neighborhood (see section 2.2.3.3).

In this study, local standardization was calculated as part of the local TOPSIS model. The raw values of the criteria were calculated using the local standardization formulas (Equations 2.13-2.14). An example of local standardization for structure year built criterion can be seen in Figure 3.10. YB_FMax represents the maximum value in each neighborhood, obtained by Focal Statistics, Year Built represents the raw values of structure year built criterion, and YearBuilt_LR represents the Local Range in each neighborhood. Structure year built is a minimization criterion and therefore Score Range formula for minimization criteria was used (Equation 2.14).

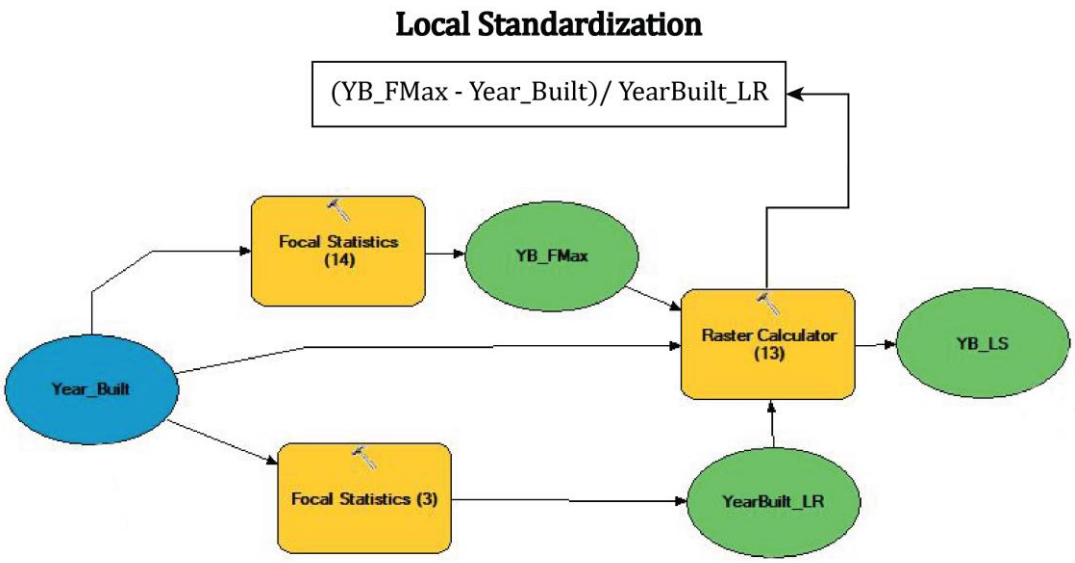

Figure 3.10. Local Standardization for structure year built (part of the local TOPSIS model).

The next step was calculating the local criterion weights. Local weighting is a function of global weight and Local Range, and can therefore be seen as a localized form of global weights (see section 2.2.3.4). Therefore, the weights produced through Pairwise Comparison (see section 3.3.5.1) were used as the global weights.

In this study local weights were calculated as part of the Local TOPSIS model. An example of local criterion weighting for structure year built, as used in the model, can be seen in Figure 3.11. Global maximum and minimum values of the criterion were obtained and were used to calculate the top fraction of Equation 2.15, where global weight is multiplied by local range and then divided by global range. Global weights were set as model parameters, meaning they had to be inserted manually when clicking on the model to run it. The second Raster calculator was used to sum the results produced in the last step. After the first raster (YearBuilt_LW1) was created, the sum of all criteria weights was calculated (Weighted_Sum). Then, the raster produced by the first Raster Calculator (YearBuilt_LW1) was divided by the sum of all weights (Weighted_Sum), in order to obtain the local weights for the criterion.

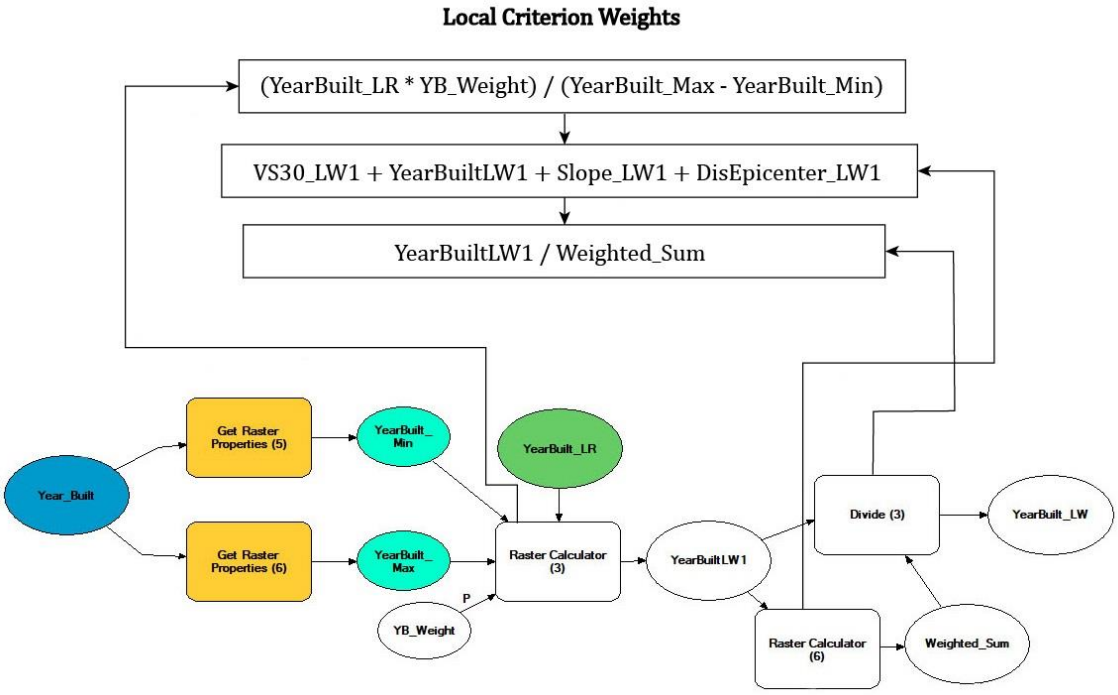

Figure 3.11. Calculation of Local Weights for structure year built (part of the local TOPSIS model).

The next step of the model included calculation of similarity to local ideal point (LIP) and similarity to local nadir point (LNP). An example of this calculation for structure year built criterion can be seen in Figure 3.12. Focal Statistics tool was used to obtain local range, LIP and LNP based on the local standardization raster (YB_LS). Then, the top Raster Calculator was used to calculate the similarity to LIP based on Equation 2.16. The bottom Raster Calculator was used to calculate similarity to LNP based on Equation 2.17.

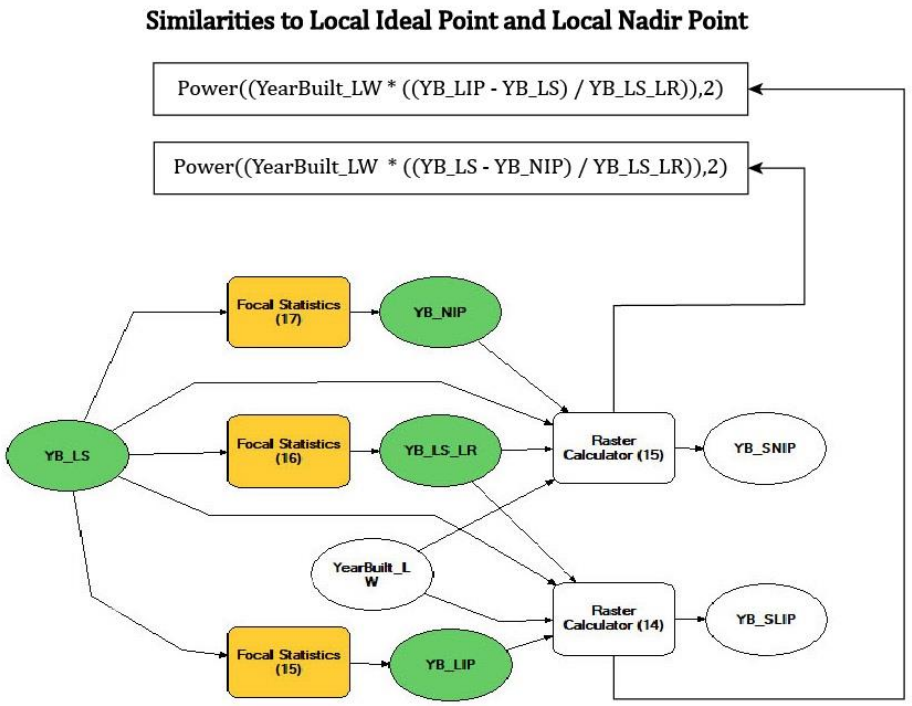

Figure 3.12. Calculation of similarities to LIP and LNP (part of the local TOPSIS model).

The last step of the model is demonstrated in Figure 3.13. Similarities to LIP and LNP were aggregated for all criteria using square root sum. Then, closeness to LIP was calculated by dividing the aggregated raster of similarity to LNP (SNIP_Sum) by the sum of the aggregated raster of similarity to LNP and the aggregated raster of similarity to LIP Equation 2.18.

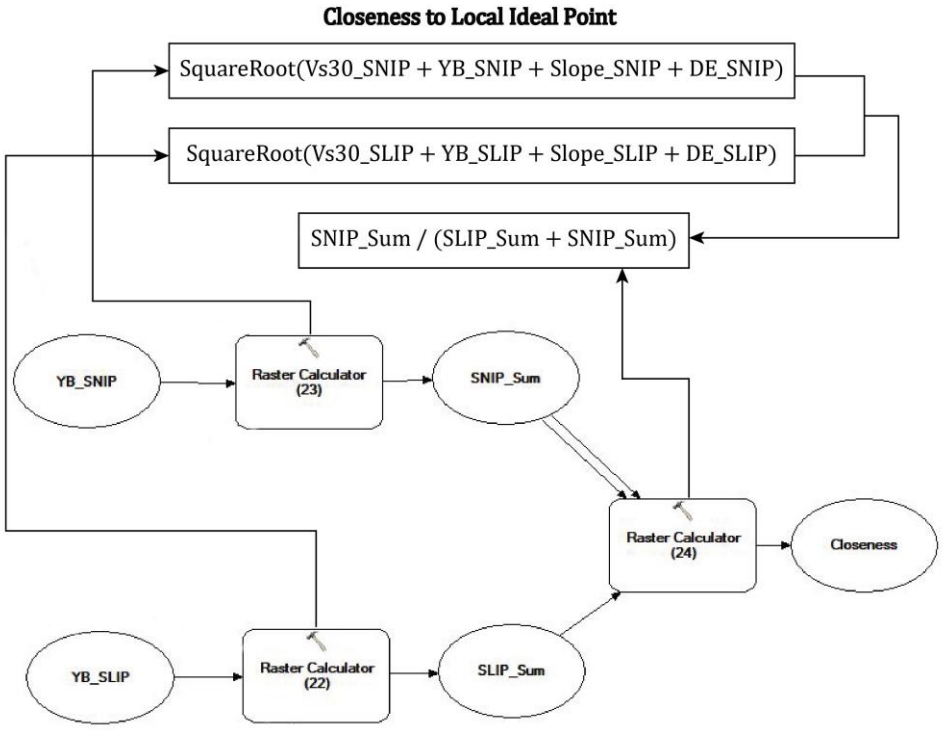

Figure 3.13. Calculation of closeness to Local Ideal Point (part of the local TOPSIS model).

3.3.6. Ranking of Alternatives and Zonal Statistics

After overall values of vulnerability levels to earthquake in the SFV were achieved, the alternatives were ranked based on their values of vulnerability. The ranking of the alternatives was performed for both Global TOPSIS and Local TOPSIS using a Python script that was created by Dr. Soheil Boroushaki (Appendix A). This script ranks the closeness to ideal point values, where rank 1 is the highest values of the closeness to ideal point raster. Then, 10 top percent of the highest ranked alternatives was calculated.

In addition, Zonal Statistics were used to calculate the average and maximum vulnerability values by census block groups based on the closeness to ideal point results produced by the two methods. The average level of vulnerability of buildings to an earthquake was calculated by first obtaining the sum of the vulnerability of all alternatives in the census block group. Then the sum was divided by the number of alternatives in the census block group. The maximum level of

vulnerability of buildings to an earthquake is based on the highest overall level of vulnerability value found in a census block group. This value is the maximum vulnerability level of the census block group in which is located.

3.4. Numerical Example

The following sections will present a decision problem involving two criteria: terrain slope (%) and proximity to water (km). Both criteria are to be minimized. The study area is in raster format and consists of 16 cells, where each cell is considered an alternative. The example criteria will be used to illustrate both the Global TOPSIS and Local TOPSIS methods.

Table 3.11. Slope criterion (%), w= 0.6.

9	10	1	1
2	4	3	2
2	5	4	0
9	4	12	10

Table 3.12. Proximity to water criterion (km), w= 0.4.

0.000	1.000	2.000	3.000
1.000	1.414	2.236	3.162
2.000	2.236	2.828	3.606
3.000	3.162	3.606	4.243

3.4.1. Global TOPSIS

Score range method was used to standardize the raw values (Tables 3.11 & 3.12) of both criteria into the same scale. Score range minimization Equation (2.4) was used to standardize the example criteria (Tables 3.13 & 3.14), as the evaluation criteria in this case were to be minimized. The standardization was based on the global range values, which is 12% for slope

and 4.243 km for proximity to water. Therefore, the criteria values were standardized as follows: $v(a_{i1}) = \frac{(12-a_{i1})}{(12-0)}$ and $v(a_{i2}) = \frac{(4.243-a_{i2})}{(4.243-0)}$, respectively.

Table 3.13. Slope criterion standardized.

0.250	0.167	0.917	0.917
0.833	0.667	0.750	0.833
0.833	0.583	0.667	1.000
0.250	0.667	0.000	0.167

Table 3.14. Proximity to water criterion - standardized.

1.000	0.764	0.529	0.293
0.764	0.667	0.473	0.255
0.529	0.473	0.333	0.150
0.293	0.255	0.150	0.000

Weights, $w_1 = 0.6$ and $w_2 = 0.4$ were assigned to slope and proximity to water criteria, respectively. In the next step, the criteria were aggregated using Global TOPSIS decision rule. The similarity to ideal point calculation (Equation 2.9) was broken into two steps. In the first step, similarity to ideal point was calculated for both criteria (Tables 3.15 & 3.18) as follows: $s_{i1} = (0.6 * \frac{1.0-v_{i1}}{1.0-0.0})^2$ and $s_{i2} = (0.4 * \frac{1.0-v_{i2}}{1.0-0.0})^2$. Then, the criteria were aggregated using square root sum: $s_i = \sqrt{s_{i1} + s_{i2}}$ (Table 3.21). The same process was performed for similarity to nadir point (Equation 2.10) for both criteria. The first step was calculated for slope and proximity to water as follows: $d_{i1} = (0.6 * \frac{v_{i1}-0.0}{1.0-0.0})^2$ and $d_{i2} = (0.4 * \frac{v_{i2}-0.0}{1.0-0.0})^2$, respectively (Tables 3.16 & 3.19). Then, the criteria were aggregated using square root sum: $d_i = \sqrt{d_{i1} + d_{i2}}$ (Table 3.22). Relative closeness to ideal point (Equation 2.11) was calculated as follows: $f_i = \frac{d_i}{s_i+d_i}$ (Table 3.17). Finally, the alternatives were ranked based on their relative closeness to ideal point (Table 3.20).

Table 3.15. Similarity to IP – slope criterion.

0.203	0.250	0.003	0.003
0.010	0.040	0.023	0.010
0.010	0.063	0.040	0.000
0.203	0.040	0.360	0.250

Table 3.16. Similarity to NP – slope criterion.

0.023	0.010	0.303	0.303
0.250	0.160	0.203	0.250
0.250	0.123	0.160	0.360
0.023	0.160	0.000	0.010

Table 3.17. Relative closeness to IP.

0.487	0.387	0.751	0.662
0.810	0.667	0.654	0.619
0.718	0.549	0.559	0.639
0.264	0.535	0.080	0.135

Table 3.18. Similarity to IP - proximity to water criterion.

0.000	0.009	0.036	0.080
0.009	0.018	0.044	0.089
0.036	0.044	0.071	0.116
0.080	0.089	0.116	0.160

Table 3.19. Similarity to NP - proximity to water criterion.

0.160	0.093	0.045	0.014
0.093	0.071	0.036	0.010
0.045	0.036	0.018	0.004
0.014	0.010	0.004	0.000

Table 3.20. Ranking of alternatives based on closeness to IP.

12	13	2	5
1	4	6	8
3	10	9	7
14	11	16	15

Table 3.21. Similarity to IP - square root sum.

0.450	0.509	0.195	0.287
0.137	0.240	0.259	0.314
0.213	0.327	0.333	0.340
0.531	0.359	0.690	0.640

Table 3.22. Similarity to NP - square root sum.

0.427	0.322	0.589	0.562
0.586	0.481	0.488	0.510
0.543	0.398	0.422	0.603
0.190	0.413	0.060	0.100

3.4.2. Local TOPSIS

A moving window of 3x3 cells was used as the neighborhood definition for the numerical example. For the Local TOPSIS method, neighborhood q=1 of both criteria was used to illustrate the method's steps. Therefore, the calculation of each step in this section was performed on focal

point *i*=1. The alternatives are represented by the letter *i*, where the alternative at the top left corner is *i*=1 and the alternative at the bottom right corner.is *i*=16. Neighborhoods located at the corners and edges of the study area, such as in Tables 3.22 and 3.23, contain cells that are located outside the study area. Considering that these cells did not contain values, they were ignored and calculations were performed based only on the remaining cells in the neighborhood.

Table 3.23. q=1 of slope criterion.

9	10	1	1
2	4	3	2
2	5	4	0
9	4	12	10

Table 3.24. q=1 of proximity to water criterion.

0.000	1.000	2.000	3.000
1.000	1.414	2.236	3.162
2.000	2.236	2.828	3.606
3.000	3.162	3.606	4.243

Local range of example criteria (Tables 3.24 & 3.25) was calculated based on Equation 2.12. An example of local range calculation for neighborhood *q*=1 of both criteria: $r_1^1 = 10 - 2 = 8$ and $r_2^1 = 1.414 - 0.0 = 1.414$.

Table 3.25. Local range for slope criterion.

8	9	9	2
8	9	10	4
7	10	12	12
7	10	12	12

Table 3.26. Local range for proximity to water criterion.

1.414	2.236	2.162	1.162
2.236	2.828	2.606	1.606
2.162	2.606	2.828	2.007
1.162	1.606	2.007	1.414

Similar to Global TOPSIS, score range method was used for local standardization. Standardization of the criteria (Tables 3.26 & 3.27) was performed based on Equation 2.14, which is used for minimization criteria. The criteria values for *q*=1 were standardized as follows:

$v_1^1 = \frac{(10-9)}{8} = 0.125$ and $v_2^1 = \frac{(1.414-0.0)}{1.414} = 1.$

Table 3.27. Local Standardized values for slope criterion.

0.125	0.000	1.000	1.000
1.000	0.667	0.700	0.500
1.000	0.700	0.667	1.000
0.000	0.800	0.000	0.167

Table 3.28. Local standardized values for proximity to water criterion.

1.000	0.553	0.538	0.140
0.553	0.500	0.526	0.276
0.538	0.526	0.500	0.318
0.140	0.276	0.318	0.000

In the next step, criterion weights were calculated based on Equation 2.15. Global weights, $w_1 = 0.6$ and $w_2 = 0.4$ were assigned to slope and proximity to water criteria, respectively. Local criterion weights calculation was performed in three steps. A calculation example of each step was given only based on *q*=1 of both criteria. The first step involved calculation of the top fraction of Equation 2.15: $w1(a_i)_1^1 = \frac{0.6*8}{12} = 0.4$ and $w1(a_i)_2^1 = \frac{0.4*1.414}{4.243} = 0.133$. In the second step, the values derived by in the first step were aggregated as follows: $\sum_k^n = 0.4 + 0.133 = 0.533$. In the third step, the local criterion weights (Tables 3.28 & 3.29) were calculated by dividing the values derived in the first step by the values derived in the second step: $w(a_i)_1^1 = \frac{0.4}{0.533} = 0.750$ and $w(a_i)_2^2 = \frac{0.133}{0.533} = 0.250.$

Table 3.29. Local Weights for slope criterion.

0.750	0.681	0.688	0.477
0.655	0.628	0.671	0.569
0.632	0.671	0.692	0.760
0.762	0.768	0.760	0.818

Table 3.30. Local weights for proximity to water criterion.

0.250	0.319	0.312	0.523
0.345	0.372	0.329	0.431
0.368	0.329	0.308	0.240
0.238	0.232	0.240	0.182

In order to calculate the Similarities to local ideal point (LIP) and local nadir point (LNP), the LIP and LNP for both criteria (Tables 3.30 - 3.33) were extracted based on the standardized values. For each alternative, the LIP was obtained by assigning the highest value in the neighborhood to the focal alternative. The same calculation was done for LNP, where the only difference was that the focal alternative was assigned the lowest values in the neighborhood.

Table 3.31. LIP for slope criterion.

1.000	1.000	1.000	1.000
1.000	1.000	1.000	1.000
1.000	1.000	1.000	1.000
1.000	1.000	1.000	1.000

Table 3.32. LNP for slope criterion.

0.000	0.000	0.000	0.500
0.000	0.000	0.000	0.500
0.000	0.000	0.000	0.000
0.000	0.000	0.000	0.000

Table 3.33. LIP for proximity to water criterion .

1.000	1.000	0.553	0.538
1.000	1.000	0.553	0.538
0.553	0.553	0.526	0.526
0.538	0.538	0.526	0.500

Table 3.34. LNP for proximity to water criterion.

0.500	0.500	0.140	0.140
0.500	0.500	0.140	0.140
0.140	0.140	0.000	0.000
0.140	0.140	0.000	0.000

The calculation of similarity to LIP for both criteria was broken into two steps. In the first step, similarity to LIP for both criteria (Tables 3.34 & 3.37) was calculated using the top part of the faction of Equation 2.16: $s_1^1 = \left(0.75 * \frac{1.0-0.125}{1.0-0.0}\right)^2 = 0.431$ and $s_2^1 = (0.25 * \frac{1.0-1.0}{1.0-0.5})^2 = 0.$ In the second step, the criteria were aggregated using square root sum (Table 3.40), based on the results of the first step: $s^1 = \sqrt{0.431 + 0} = 0.656$. The same steps were applied for the calculation of similarity to nadir point. In the first step, similarity to nadir point was calculated for both criteria (Tables 3.35 & 3.38) using the top fraction of Equation 2.17:

$d_1^1 = \left(0.75 * \frac{0.125-0.0}{1.0-0.0}\right)^2 = 0.009$ and $d_2^1 = (0.25 * \frac{1.0-0.5}{1.0-0.5})^2 = 0.062$. In the second step, the criteria were aggregated using square root sum (Table 3.41), based on the results of the first step: $d^1 = \sqrt{0.009 + 0.062} = 0.267$. Then relative closeness to ideal point (Table 3.36) was calculated as follows (Equation 2.18): $f^1 = \frac{0.267}{0.656+0.267} = 0.289$. Lastly, the alternatives were ranked based on their relative closeness to local ideal point (Table 3.39).

Table 3.35. Similarity to LIP ideal point for Slope criterion.

0.431	0.464	0.000	0.000
0.000	0.044	0.040	0.324
0.000	0.040	0.053	0.000
0.580	0.024	0.578	0.465

Table 3.36. Similarity to LNP for proximity to water criterion.

0.062	0.001	0.090	0.000
0.001	0.000	0.095	0.022
0.126	0.095	0.086	0.021
0.000	0.006	0.021	0.000

Table 3.37. Relative closeness to LIP.

0.289	0.044	0.985	0.477
0.680	0.495	0.735	0.189
0.982	0.735	0.703	0.891
0.000	0.741	0.159	0.162

Table 3.38. Similarity to LIP for Proximity to Water criterion.

0.000	0.081	0.000	0.273
0.095	0.138	0.000	0.080
0.000	0.000	0.000	0.009
0.057	0.023	0.009	0.033

Table 3.39. Similarity to LNP for proximity to water criterion.

0.062	0.001	0.090	0.000
0.001	0.000	0.095	0.022
0.126	0.095	0.086	0.021
0.000	0.006	0.021	0.000

Table 3.40. Ranking of alternatives based on closeness to LIP.

11	15	1	10
8	9	5	12
2	5	7	3
16	4	14	13

Table 3.41. Similarity to LIP - square root sum.

0.656	0.738	0.012	0.523
0.309	0.427	0.202	0.636
0.014	0.202	0.231	0.095
0.798	0.217	0.766	0.706

Table 3.42. Similarity to LNP- square root sum.

0.267	0.034	0.751	0.477
0.656	0.419	0.561	0.148
0.725	0.561	0.547	0.774
0.000	0.619	0.145	0.136

4. Results

This chapter will describe the results produced by the two methodologies, Local TOPSIS and Global TOPSIS, used to calculate the level of physical vulnerability of buildings in the SFV to earthquakes

4.1. Global TOPSIS

4.1.1. Closeness to Ideal (Vulnerable) Point

In this study, closeness to ideal point can also be described as closeness to most vulnerable point. As demonstrated by the map (Figure 4.1), the relative closeness to ideal or vulnerable point through Global TOPSIS shows higher levels of vulnerability to an earthquake in areas that are located closer to the epicenter. In the SFV, therefore, buildings in the northern area of the SFV have higher vulnerability due to being closer to the epicenter. The data shows a pattern of decreasing levels of vulnerability for buildings as distance from the epicenter increases. Therefore, buildings in the southern part of the SFV have lower risk levels. This pattern is also validated by ranking of top 10% of the closeness to ideal point values (Figure 4.2). It can be noticed that the top 10% of vulnerability values are only located at the northern part of the SFV, close to the epicenter and do not exist in other areas.

In Global TOPSIS, distance to the epicenter criterion was assigned the highest weight (Table 3.3). Therefore, using this method, distance to the epicenter has the most impact on level of vulnerability (Figure 3.2). Slope criterion was assigned the second highest weight. Therefore, higher levels of slope, especially in the north-west parts of the SFV, contribute to higher levels of vulnerability of buildings. There are also areas in the west and south-west parts of the SFV that

have moderately higher levels of vulnerability for buildings, compared to other cells in these areas. This is because these areas have steeper slopes in comparison with other areas in the same vicinity. As previously mentioned, older buildings generally have higher level of vulnerability (see section 2.4.3). However, because structure year built criterion was assigned relatively small weight, the results of Global TOPSIS do not represent this. Therefore, although some areas of the south-east part of the SFV (Burbank and Glendale) have higher concentrations of older buildings, these areas do not present with high levels of vulnerability according to this method (Figure 3.4).

Average shear wave velocity was assigned the smallest weight in Global TOPSIS, therefore having very small impact on the calculations. High levels of average shear wave velocity were associated with lower levels of vulnerability of buildings (see section 2.4.2). However, even though the northern areas of the SFV have higher levels of average shear wave velocity (Figure 3.3), it did not reduce the level of vulnerability because of the low weight assigned to the criterion. Similarly, there are areas in the southern part of the center of the SFV which have low average shear wave velocity; however vulnerability levels remained low due to the small weight of the criterion.

Figure 4.1. Vulnerability of buildings to an earthquake (Santa Susana Fault scenario) calculated by closeness to ideal point through Global TOPSIS.

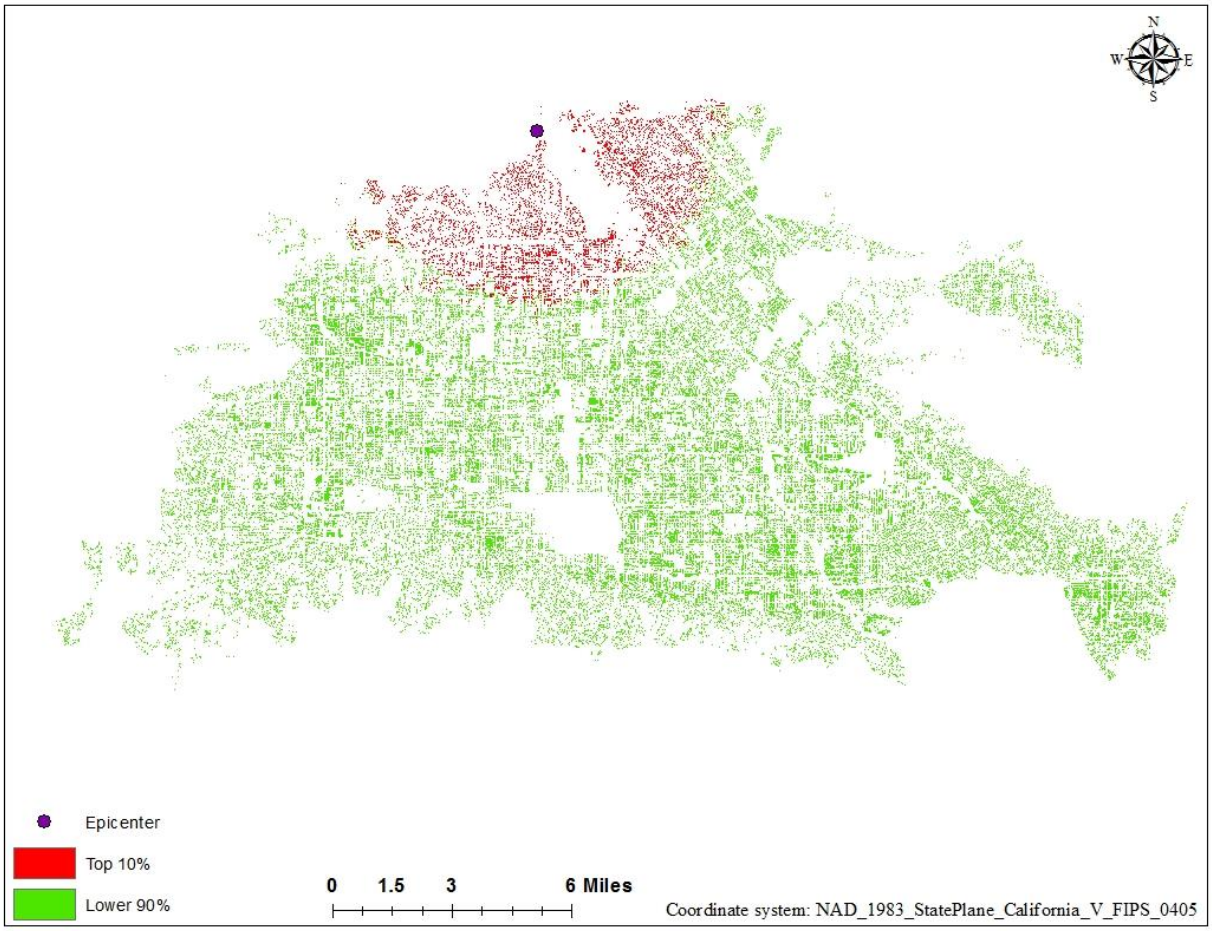

Figure 4.2. Top 10% of ranked values based on Global TOPSIS' closeness to ideal point.

4.1.2. Zonal Statistics

The average level of vulnerability shows the same pattern of higher vulnerability rates for buildings located at the northern part of the SFV, close to epicenter (Figure 4.3). The census block group with the highest average level of vulnerability of buildings is 060371066411 (FIPS) with average level of 0.606.

Maximum levels of vulnerability of buildings by census block groups (Figure 4.4) show a general pattern of higher vulnerability of buildings closer to the epicenter, but it is also noticed that there are some block groups with high maximum values at the southern margins of the SFV,

west of Encino. This can be attributed to the higher levels of slope in this area and to the relative high weight of slope in this analysis.

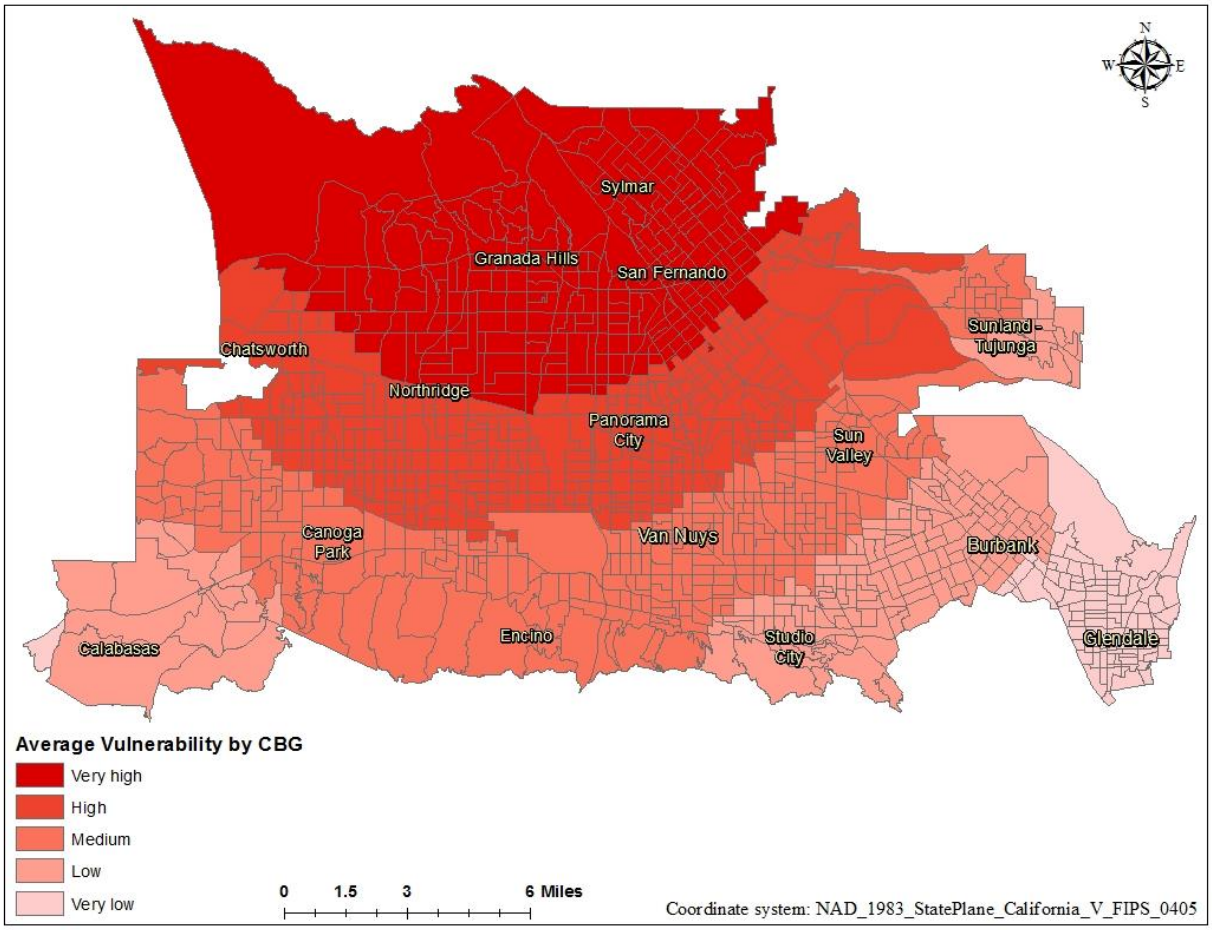

Figure 4.3. Average vulnerability of buildings by census block groups (CBG) to an earthquake for the SFV calculated based on closeness to ideal point through Global TOPSIS.

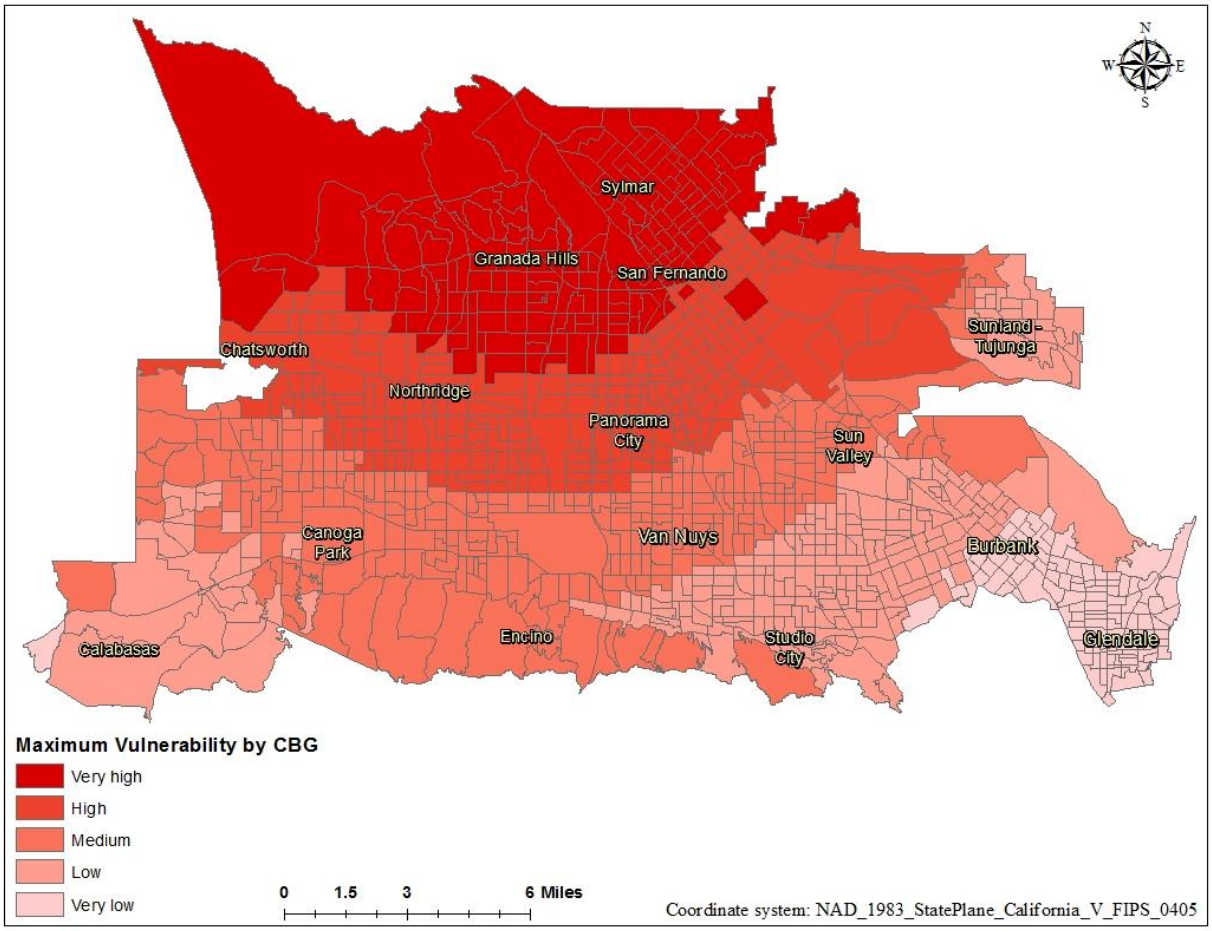

Figure 4.4. Maximum vulnerability of buildings by CBG to an earthquake for the SFV calculated based on closeness to ideal point through Global TOPSIS.

4.2. Local TOPSIS

4.2.1. Closeness to Ideal (Vulnerable) Point

Closeness to ideal point through Local TOPSIS shows less of a pattern in level of vulnerability of buildings (Figure 4.10). High levels of vulnerability, as seen in the top 10 percent of closeness to ideal point map (Figure 4.11), are located throughout the SFV. This variability can be explained by the fact that local weights take into consideration the range of values in each neighborhood. Within neighborhoods, criteria that have larger ranges are assigned higher weights in Local TOPSIS. Distance to the epicenter does not have large variability within

a neighborhood, because the buildings in that neighborhood will have similar distances to the epicenter, therefore the range of the values on the neighborhood scale are small, and thus the weights assigned are low (Figure 4.12). Structure year built, however, has large range within a neighborhood, therefore in Local TOPSIS a big amount this criterion's cells were assigned high weights (Figure 4.13), and therefore areas with larger ranges in year built show higher levels of vulnerability of buildings. In the few areas where slope and average shear wave velocity have sudden large ranges in values, higher weights were assigned, and therefore vulnerability levels were higher. In most of the study area there are not sudden changes in values for average shear wave velocity and therefore low weights were assigned to most cells in those criteria (Figure 4.14). For slope criterion it is evident that higher weights were assigned at the base of the mountains and hills surrounding the SFV (Figure 4.15), where there are sudden changes in slope values (Figure 3.4).

Figure 4.5. Vulnerability of buildings to an earthquake (Santa Susana Fault scenario) calculated by closeness to ideal point through Local TOPSIS.

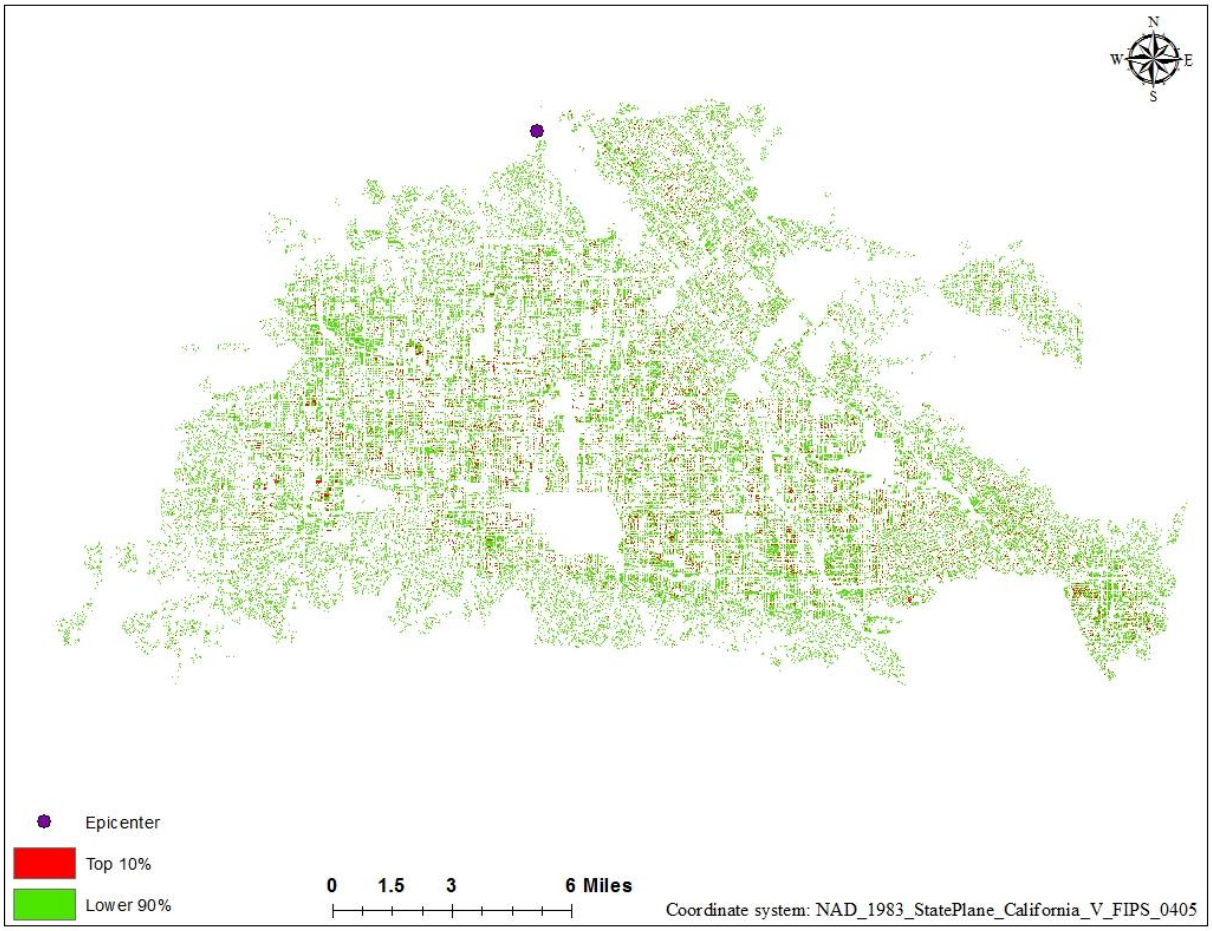

Figure 4.6. Top 10% of ranked values based on Global TOPSIS' closeness to ideal point.

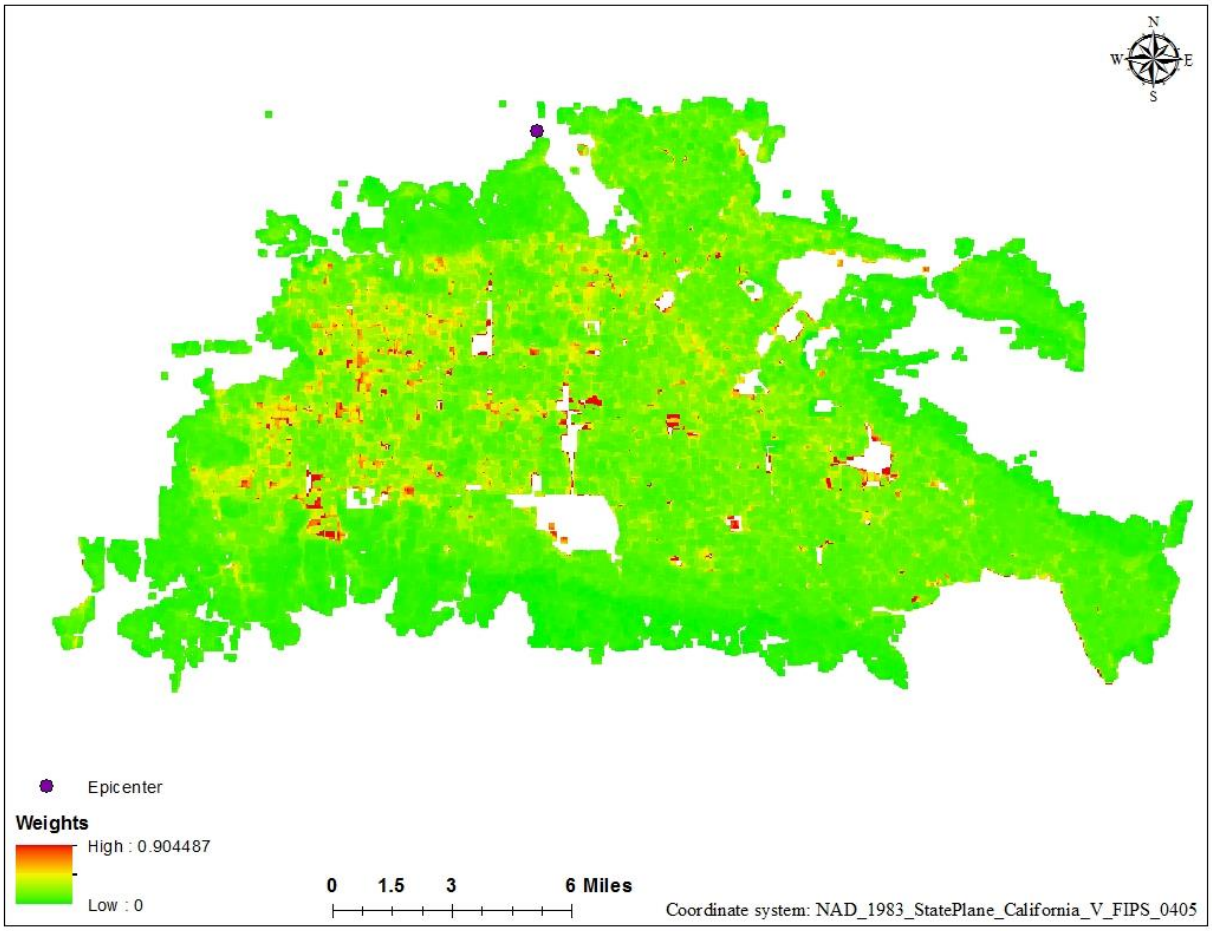

Figure 4.7. Local weights for distance to epicenter criterion.

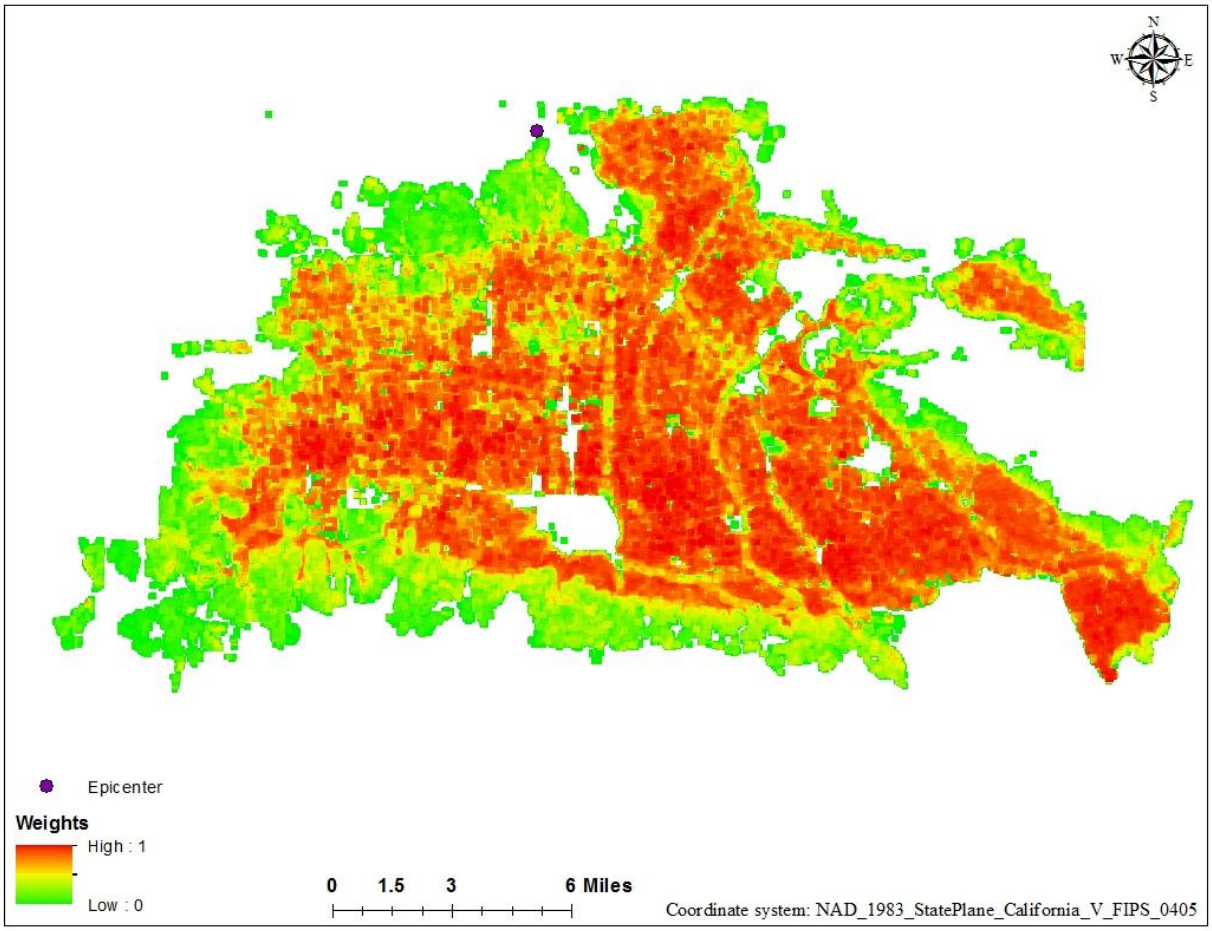

Figure 4.8. Local weights for structure year built criterion.

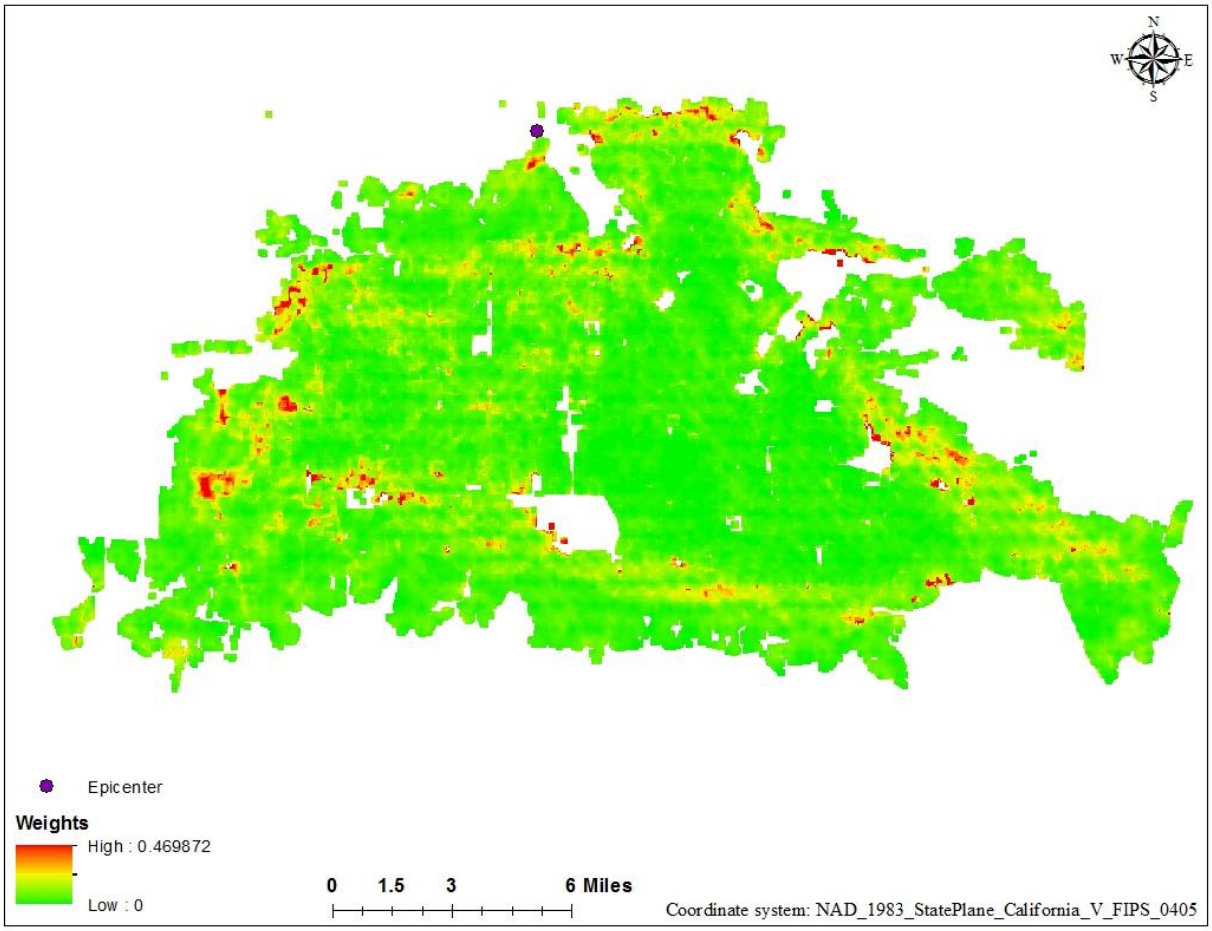

Figure 4.9. Local weights for average shear wave velocity criterion.

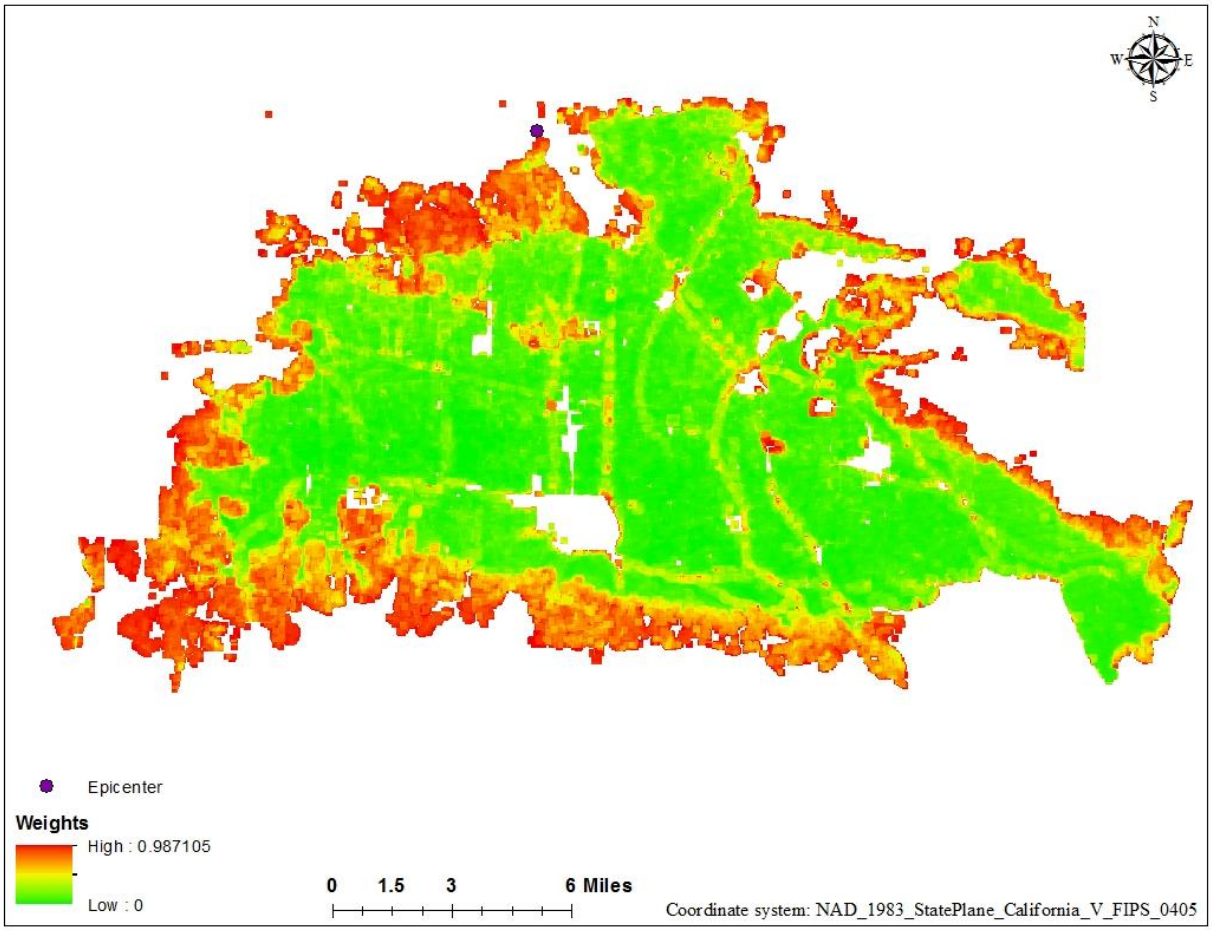

Figure 4.10. Local weights for slope criterion.

4.2.2. Zonal Statistics

The average level of vulnerability by census block groups (Figure 4.16) shows higher level of average vulnerability in census block groups that have a large number of old buildings (Figure 3.3). This also is due to the fact that year built was assigned the highest criterion weights through local weights process. Similar to the calculations in Global TOPSIS, the maximum level of vulnerability of a census block was assigned based on that block's highest cell value of vulnerability.

High levels of maximum vulnerability of buildings to earthquakes are common throughout the study area (Figure 4.17) because there are a lot of neighborhoods in the SFV with many old

buildings, especially in places such as North Hollywood, Glendale, and Sylmar. Other census block groups with high maximum vulnerability level of buildings, such as in Calabasas and Tarzana, can also be explained by the amount of older buildings, but also by drastic changes in slope values and average shear wave velocities (Figures 3.4 and 3.5).

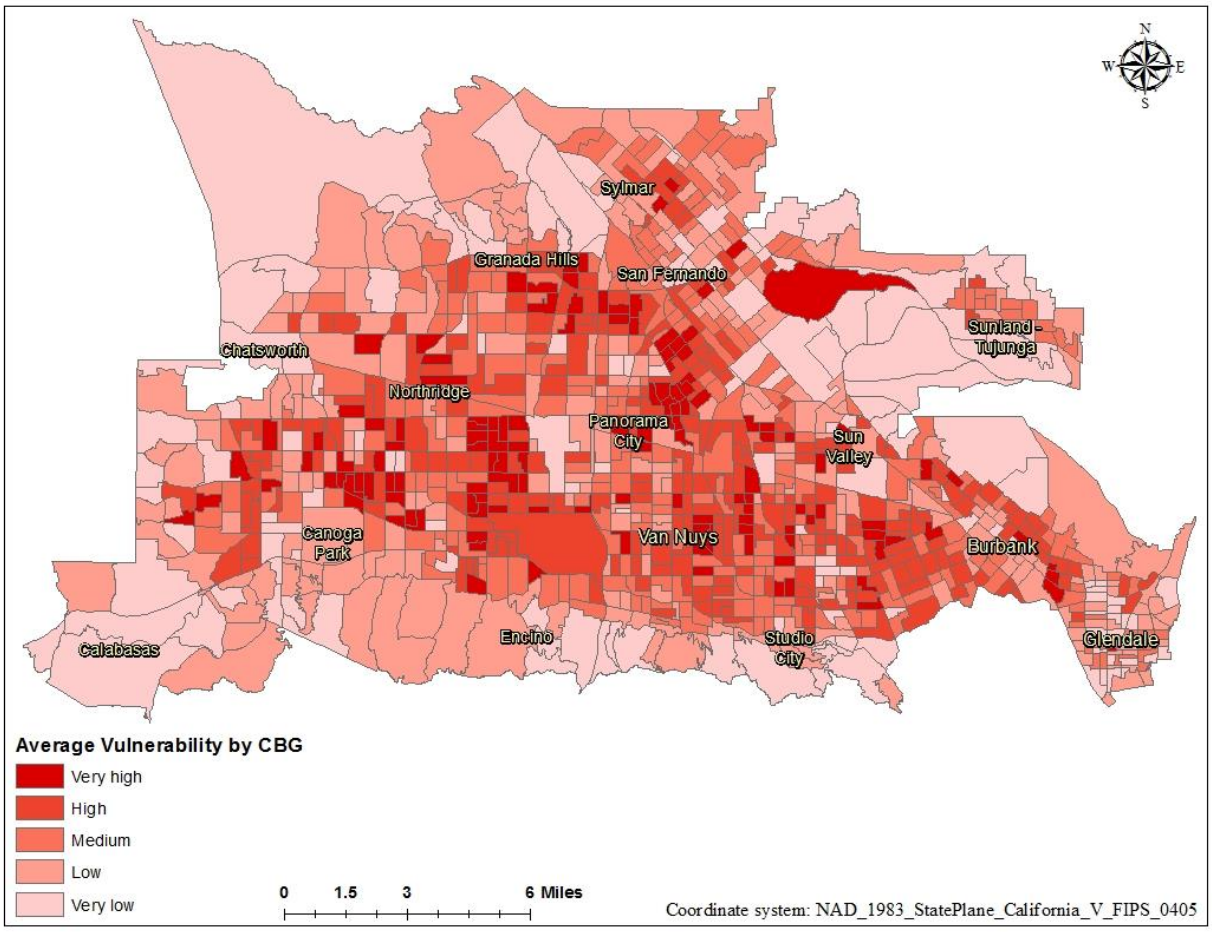

Figure 4.11. Average vulnerability of buildings by CBG to an earthquake for the SFV calculated based on closeness to ideal point through Local TOPSIS.

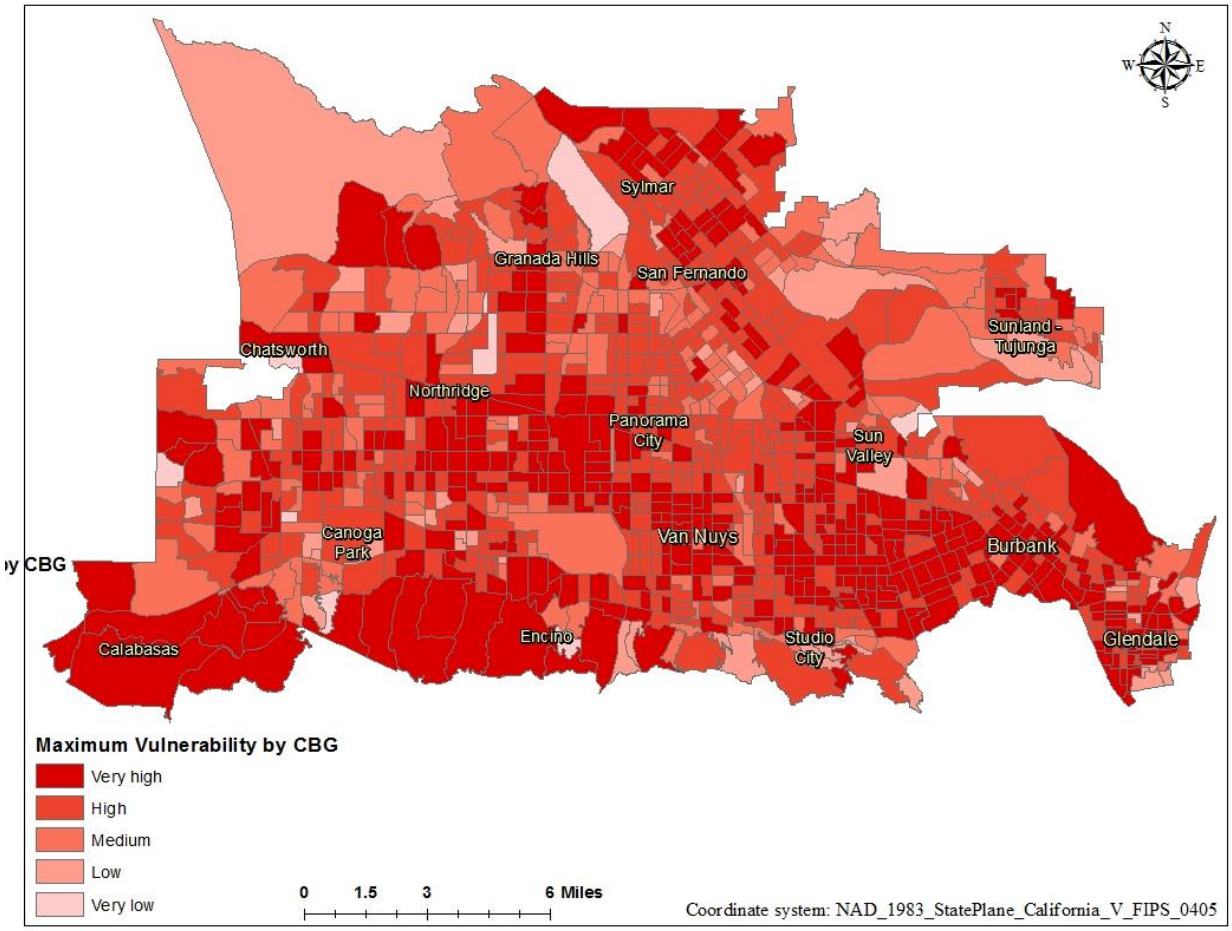

Figure 4.12. Maximum vulnerability of buildings by CBG to an earthquake for the SFV calculated based on closeness to ideal point through Local TOPSIS.

5. Discussion

This chapter will discuss the impact of the level of vulnerability of buildings to earthquakes on the Santa Susana fault based on data outcomes from both Global TOPSIS and Local TOPSIS methods. In addition, the advantages and disadvantages of each method will be discussed in relation to assessment of vulnerability to earthquakes.

Based on the outcomes of the data from the Global TOPSIS method, the areas with the highest levels of vulnerability of buildings are located in the northern part of the SFV with short distance to the epicenter. This can be attributed largely to the fact the highest weights were assigned to distance to the epicenter criterion through Pairwise Comparison technique. This also is due to some parts of this area also having relatively steep slopes, which is the criterion that was assigned the second highest weight. Owing to the way that weights are distributed in this method, factors with low weights were not significantly reflected in the results, even though these factors are known to impact levels of vulnerability of buildings.

Table 5.1. Census block groups with the highest average vulnerability levels based on Global TOPSIS. Population source: U.S. Census Bureau 2015.

FIPS	Neighborhood/City	Vulnerability level	Population
060371066411	LA City - Granada Hills	0.605883	2,145
060371066421	LA City - Granada Hills	0.603815	1,330
060371066431	LA City - Granada Hills	0.603744	3,077
		Total Population	6,552

Table 5.2. Census block groups with the highest maximum vulnerability levels based on Global TOPSIS. Population source: U.S. Census Bureau 2015.

FIPS	Neighborhood/City	Vulnerability level	Population
060371081021	LA City - Porter Ranch	0.684073	3,706
060371066032	LA City - Granada Hills	0.666127	1,761
060371066431	LA City - Granada Hills	0.660063	3,077
		Total Population	8,544

Using the Global TOPSIS method to analyze the data, the three census block groups with the highest average vulnerability levels are located in Granada Hills. The total population in these three census block groups is 6,552 (Table 5.1). This is the amount of people living in areas that are at high risk of experiencing significant damage during an earthquake scenario with the epicenter located on the Santa Susana fault. The census block groups with the highest maximum vulnerability levels of buildings are located in Granada Hills and Porter Ranch. The total population in these three census block groups is 8,544. (Table 5.2)

Based on the outcomes of the data analysis from the Local TOPSIS method, areas with high levels of vulnerability of buildings are located in areas with a big range of years in which structures were built. This can be attributed to the range sensitivity principle in the Local TOPSIS method. Therefore, for each criterion, weights are assigned based on the range of values in the neighborhood. Owing to the year built criterion having the largest range in values across a geographical space, it was assigned the highest weight in this method. Contrary to Global TOPSIS, in the Local TOPSIS method, distance to the epicenter criterion was assigned the lowest weights due to the small range of values within a geographical space. In this method, slope has moderate significance on the vulnerability levels, especially in areas with higher levels of slope which are located next to areas with low levels of slope.

Table 5.3. Census block groups with the highest average vulnerability levels based on Local TOPSIS. Population source: U.S. Census Bureau 2015.

FIPS	Neighborhood/City	Vulnerability level	Population
060371313003	LA City - Reseda	0.781081	1,480
060371237002	LA City - Valley Glen	0.777065	881
060371210201	LA City - Sun Valley	0.770261	1,047
		Total Population	3,408

Table 5.4. Census block groups with the highest maximum vulnerability levels based on Local TOPSIS. Population source: U.S. Census Bureau 2015.

FIPS	Neighborhood/City	Vulnerability level	Population
060373017022	Glendale	0.996393	1,579
060371231031	LA City - North Hollywood	0.995692	1,625
060371221201	LA City - Sun Valley	0.996424	2,396
		Total Population	5,600

Using the Local TOPSIS method, the census block groups with the highest average vulnerability levels are located in Reseda, Valley Glen and Sun Valley. The total population of these three census block groups is 3,408 (Table 5.3). The census block groups with the highest maximum vulnerability levels of buildings are located in Glendale, North Hollywood and Sun Valley. The total population of these census block groups is 5,600 (Table 5.4).

Based on the literature, areas which are located closer to the epicenter of an earthquake have higher risk of damage. Therefore, the Global TOPSIS method yields a more accurate picture of assessment of vulnerability to earthquakes. However, even though this important criterion is heavily weighted, Global TOPSIS does not give significance to other important factors which can impact building risk, such as the age of the structure, slope, and average shear wave velocity. It is important to consider other factors in calculating vulnerability. For example, areas with higher slope values are more susceptible to landslides during an earthquake. Additionally, newer buildings are constructed according to seismic code, making them less susceptible to major damage in an earthquake, whereas older buildings were not built to this code, therefore making them at greater risk for damage. Comparatively, Local TOPSIS assigns weights based on theory rather than subjective assignments. Therefore, the data that the criteria contain have high importance in the outcome of the MCDA process.

Though Local TOPSIS assigns weights in a more effective manner, it also has disadvantages. One of these disadvantages is that distance to epicenter, which is an important factor in calculating risk, is assigned a low weight owing to the small range of this criterion on a neighborhood scale. In addition, criteria which have the same value over a large continuous space, thereby having a range value of zero in a large number of neighborhoods, cause data loss when calculating local weights due to the inability to divide by zero. Therefore, some important factors, such as soil type, cannot be used efficiently in MCDA that uses Local TOPSIS method. In case of use of criteria that have moderate change in values over an area, such as structure year built, different neighborhood sizes need to be tested through Local TOPSIS process. These tests will be used to identify the neighborhood size which is large enough to prevent significant data loss, while also maintaining a small enough size so that local factors will still be significant in the analysis. Small neighborhood size is important in order to be able to use detailed local information and peak values.

6. Conclusion

This study compared the use of MCDA methods: Global TOPSIS and Local TOPSIS for assessing vulnerability of buildings to earthquakes in the SFV. The Global model indicates an overall spatial pattern for the whole study area, which is much dependent on weights assigned to criteria subjectively. The Local model generates a more dispersed distribution of values within the study area. Range sensitivity principle dictates weights distribution for the Local model. Based on the literature review, the results of Global TOPSIS show a better reflection of predicted vulnerability of buildings to earthquakes. With that said, Local TOPSIS is a very efficient MCDA method when the decision problem contains criteria with big ranges in values over small geographical scale. Both methods would yield more accurate results if there was data available that could be used as additional study criteria. Vulnerability levels of buildings to earthquakes are dependent on many factors that can vary from building to building, and each factor must be taken into consideration when deriving a risk level. Although the study did not consider every factor due to data availability, the results, especially those produced by Local TOPSIS method, can be used in the development of mitigation plans and preventative measures for updating older buildings to meet seismic codes.

References

Aghataher, R., Delavar, M. R., Nami, M. H., & Samnay, N. (2008). A fuzzy-AHP decision support system for evaluation of cities vulnerability against earthquakes. *World Applied Sciences Journal*, *3*(1), 66-72.

Ahmed, M. M., Jahan, I., & Alam, M. J. (2014). Earthquake vulnerability assessment of existing buildings in cox's-bazar using field survey & GIS. *International Journal of Engineering*, *3*(8).

Anbazhagan, P., Thingbaijam, K. K. S., Nath, S. K., Kumar, J. N., & Sitharam, T. G. (2010). Multi-criteria seismic hazard evaluation for Bangalore city, India. *Journal of Asian Earth Sciences*, *38*(5), 186-198.

Armaş, I. (2012). Multi-criteria vulnerability analysis to earthquake hazard of Bucharest, Romania. *Natural hazards*, *63*(2), 1129-1156.

Barbat, A. H., Pujades, L. G., & Lantada, N. (2006). Performance of buildings under earthquakes in Barcelona, Spain. *Computer‐Aided Civil and Infrastructure Engineering*, *21*(8), 573-593.

Brown, L. T., Diehl, J. G., & Nigbor, R. L. (2000, February). A simplified procedure to measure average shear-wave velocity to a depth of 30 meters (VS30). In Proceedings of 12th world conference on earthquake engineering.

Cochrane, S. W., & Schaad, W. H. (1992). Assessment of earthquake vulnerability of buildings. In *Tenth World Conference on Earthquake Engineering* (Vol. 1, pp. 497-502).

Cova, T. J. (1999). GIS in emergency management. *Geographical information systems*, *2*, 845-858.

Crowley, H., Pinho, R., & Bommer, J. J. (2004). A probabilistic displacement-based vulnerability assessment procedure for earthquake loss estimation. *Bulletin of Earthquake Engineering*, *2*(2), 173-219.

DeCourten, F. (2006). Geology of Southern California.

Encyclopædia Britannica (2011). *San Fernando Valley*. https://www.britannica.com/place/San-Fernando-Valley (last accessed 1 October 2017).

Erden, T., & Karaman, H. (2012). Analysis of earthquake parameters to generate hazard maps by integrating AHP and GIS for Küçükçekmece region. *Natural Hazards and Earth System Sciences*, *12*(2), 475-483.

Delavar, M. R., Moradi, M., & Moshiri, B. (2015). Earthquake Vulnerability Assessment for Hospital Buildings Using a Gis-Based Group Multi Criteria Decision Making Approach: a Case Study of Tehran, Iran. *The International Archives of Photogrammetry, Remote Sensing and Spatial Information Sciences*, *40*(1), 153.

Dolan, J. F., Gath, E. M., Grant, L. B., Legg, M., Lindvall, S., Mueller, K., Oskin, M., Ponti, D. F., Rubin. C. M., Rockwell, T. K., Shaw, J. H., Treiman, J. A., Walls, C. & Yeats R. S. (complier) (2001). Active faults in the Los Angeles metropolitan region. *SCEC Special Publication Series.*

FEMA (2017). *Building Codes*. https://www.fema.gov/building-codes (last accessed 24 Novermber 2017).

FEMA (n.d.). *Effect of Soil and Rock Types*. https://training.fema.gov/emiweb/earthquake/neh0102320.htm (last accessed 24 Novermber 2017).

Field, E. H. (2015). *UCERF3: A new earthquake forecast for California's complex fault system* (No. 2015-3009). US Geological Survey.

Ghazvini, T., Tavakoli, H. R., Neya, B. N., & Sarokolayi, L. K. (2013). Seismic response of aboveground steel storage tanks: comparative study of analyses by six and three correlated earthquake components. Latin American Journal of Solids and Structures, 10(6), 1155-1176.

Hack, R., Alkema, D., Kruse, G. A., Leenders, N., & Luzi, L. (2007). Influence of earthquakes on the stability of slopes. *Engineering geology*, *91*(1), 4-15.

Hizbaron, D. R., Baiquni, M., Sartohadi, J., Rijanta, R., & Coy, M. (2011). Assessing social vulnerability to seismic hazard through spatial multi criteria evaluation in Bantul District, Indonesia. In *Conference of Development on the Margin, Tropentag*.

Hwang, C. L., & Yoon, K. (1981). Methods for multiple attribute decision making. In *Multiple attribute decision making* (pp. 58-191). Springer Berlin Heidelberg.

IRIS and University of Portland (n.d.). Buildings and earthquakes—Which stands? Which falls? http://www.iris.edu/hq/files/programs/education_and_outreach/retm/tm_100112_haiti/BuildingsInEQs_2.pdf (last accessed 15 November 2016).

Karapetrou, S. T., Fotopoulou, S. D., & Pitilakis, K. D. (2015). Seismic vulnerability assessment of high-rise non-ductile RC buildings considering soil–structure interaction effects. *Soil Dynamics and Earthquake Engineering*, *73*, 42-57.

Karimzadeh, S., Miyajima, M., Hassanzadeh, R., Amiraslanzadeh, R., & Kamel, B. (2014). A GIS-based seismic hazard, building vulnerability and human loss assessment for the earthquake scenario in Tabriz. *Soil Dynamics and Earthquake Engineering*, *66*, 263-280.

Keefer, D. K. (1984). Landslides caused by earthquakes. *Geological Society of America Bulletin*, *95*(4), 406-421.

Levi, T., Bausch, D., Katz, O., Rozelle, J., & Salamon, A. (2015). Insights from Hazus loss estimations in Israel for Dead Sea Transform earthquakes. *Natural Hazards*, *75*(1), 365-388.

Los Angeles County GIS Data Portal (2016). *CENSUS_BLOCK_GROUPS*. https://egis3.lacounty.gov/dataportal/2016/01/26/census_block_groups/ (last accessed 17 October 2017).

Los Angeles County GIS Data Portal (2016). *Countywide Building Outlines – 2014 Update – Public Domain Release*. https://egis3.lacounty.gov/dataportal/2016/11/03/countywide-building-outlines-2014-update-public-domain-release/ (last accessed 18 October 2017).

Lowrie, W. (2007). *Fundamentals of geophysics*. Cambridge university press.

Lu, G. Y., & Wong, D. W. (2008). An adaptive inverse-distance weighting spatial interpolation technique. Computers & Geosciences, 34(9), 1044-1055.

Malczewski, J. (1999). *GIS and multicriteria decision analysis*. John Wiley & Sons.

Malczewski, J. (2004). GIS-based land-use suitability analysis: a critical overview. *Progress in planning*, *62*(1), 3-65.

Malczewski, J. (2011). Local weighted linear combination. *Transactions in GIS*, *15*(4), 439-455.

Malczewski, J., & Rinner, C. (2015). *Multicriteria decision analysis in geographic information science*. Springer.

Martins, V. N., e Silva, D. S., & Cabral, P. (2012). Social vulnerability assessment to seismic risk using multicriteria analysis: the case study of Vila Franca do Campo (Sao Miguel Island, Azores, Portugal). *Natural hazards*, *62*(2), 385-404.

Menoni, S., Pergalani, F., Boni, M. P., & Petrini, V. (2002). Lifelines earthquake vulnerability assessment: a systemic approach. *Soil Dynamics and Earthquake Engineering*, *22*(9), 1199-1208.

Moffatt, S. F., & Cova, T. J. (2010). Parcel-scale earthquake loss estimation with HAZUS: a case study in Salt Lake County, utah. *Cartography and Geographic Information Science*, *37*(1), 17-29.

Moore, J. R., Gischig, V., Amann, F., Hunziker, M., & Burjanek, J. (2012). Earthquake-triggered rock slope failures: Damage and site effects. In *Proceedings 11th International & 2nd North American Symposium on Landslides*.

Moustafa, S. S. (2015). Application of the Analytic Hierarchy Process for Evaluating Geo-Hazards in the Greater Cairo Area, Egypt. *Electronic Journal of Geotechnical Engineering*, *20*, 1921-1938.

Murty, C. V. R., Rupen Goswami, V. A., & Vipul, V. M. (2013). Some Concepts in Earthquake Behaviour of Buildings. *Gujarat State Disaster Management Authority, Government of Gujarat*.

Nelson, S. A. (2013). *Slope Stability, Triggering Events, Mass Movement Hazards*. http://www.tulane.edu/~sanelson/Natural_Disasters/slopestability.htm (last accessed 22 October 2017).

Otani, S. (2000). Seismic vulnerability assessment of reinforced concrete buildings. *RECON no. 20010104150.; Journal of the School of Engineering, the University of Tokyo*, *47*, 5-2.

Panahi, M., Rezaie, F., & Meshkani, S. A. (2014). Seismic vulnerability assessment of school buildings in Tehran city based on AHP and GIS. *Natural Hazards and Earth System Sciences*, *14*(4), 969-979.

Ploeger, S. K., Atkinson, G. M., & Samson, C. (2010). Applying the HAZUS-MH software tool to assess seismic risk in downtown Ottawa, Canada. *Natural hazards*, *53*(1), 1-20.

Pollino, M., Fattoruso, G., La Porta, L., Della Rocca, A. B., & James, V. (2012). Collaborative open source geospatial tools and maps supporting the response planning to disastrous earthquake events. *Future Internet*, *4*(2), 451-468.

Qin, X. (2013). Local ideal point method for GIS-based multicriteria analysis: A case study in London, Ontario.

Rashed, T., & Weeks, J. (2003). Assessing vulnerability to earthquake hazards through spatial multicriteria analysis of urban areas. *International Journal of Geographical Information Science*, *17*(6), 547-576.

Saaty, T. L. (1994). How to make a decision: the analytic hierarchy process. *Interfaces*, *24*(6), 19-43.

Saaty, T. L. (2008). Decision making with the analytic hierarchy process. *International journal of services sciences*, *1*(1), 83-98.

Servi, M. (2004). *Assessment of vulnerability to earthquake hazards using spatial multicriteria analysis: Odunpazari, Eskisehir case study* (Doctoral dissertation, MIDDLE EAST TECHNICAL UNIVERSITY).

Sheikhian, H., Delavar, M. R., & Stein, A. (2015). Integrated estimation of seismic physical vulnerability of Tehran using rule based granular computing. *The International Archives of Photogrammetry, Remote Sensing and Spatial Information Sciences*, *40*(3), 187.

Southern California Earthquake Data Center (2013 a). *Significant Earthquakes and Faults - Sierra Madre Fault Zone*. http://scedc.caltech.edu/significant/sierramadre.html (last accessed 1 November 2017).

Southern California Earthquake Data Center (2013 b). *Significant Earthquakes and Faults - Santa Susana Fault Zone*. http://scedc.caltech.edu/significant/santasusana.html (last accessed 1 November 2017).

State of California – Department of Conservation (2017). *California State Plane Coordinate System.* http://www.conservation.ca.gov/cgs/information/geologic_mapping/state_plane (last accessed 20 October 2017).

Triantaphyllou, E., & Lin, C. T. (1996). Development and evaluation of five fuzzy multiattribute decision-making methods. *International Journal of Approximate Reasoning*, *14*(4), 281-310.

Tucker, B. E., Erdik, M. Ö., & Hwang, C. N. (Eds.). (2013). *Issues in urban earthquake risk* (Vol. 271). Springer Science & Business Media.

Twiss, R. J., & Moores, E. M. (1992). *Structural geology*. Macmillan.

Uitto, J. I. (1998). The geography of disaster vulnerability in megacities: a theoretical framework. *Applied geography*, *18*(1), 7-16.

United Nations, (1991). Mitigating Natural Disasters: Phenomena, Effects, and Options: a Manual for Policy Makers and Planners (New York: UNDRO (United Nations Disaster Relief Organization).

U.S. Census Bureau (2015). Total Population, Universe: Total population, 2011-2015 American Community Survey 5-Year Estimates. https://factfinder.census.gov/faces/tableservices/jsf/pages/productview.xhtml?pid=ACS_15_5YR_B01003&prodType=table (last accessed 02 November 2017).

U.S. Geological Survey (n.d. a). *Earthquake Facts & Earthquake Fantasy*. https://earthquake.usgs.gov/learn/topics/megaqk_facts_fantasy.php (last accessed 05 December 2016).

U.S. Geological Survey (n.d. b). *Vs30 Models and Data*. https://earthquake.usgs.gov/data/vs30/ (last accessed 17 October 2017).

U.S. Geological Survey (2017). *National Elevation Dataset*. https://viewer.nationalmap.gov/basic/?basemap=b1&category=ned,nedsrc&title=3DEP%20View (last accessed 21 October 2017).

Walker, B. B., Taylor-Noonan, C., Tabbernor, A., Bal, H., Bradley, D., Schuurman, N., & Clague, J. J. (2014). A multi-criteria evaluation model of earthquake vulnerability in Victoria, British Columbia. *Natural hazards*, *74*(2), 1209-1222.

Appendix A

Global TOPSIS ArcGIS Model

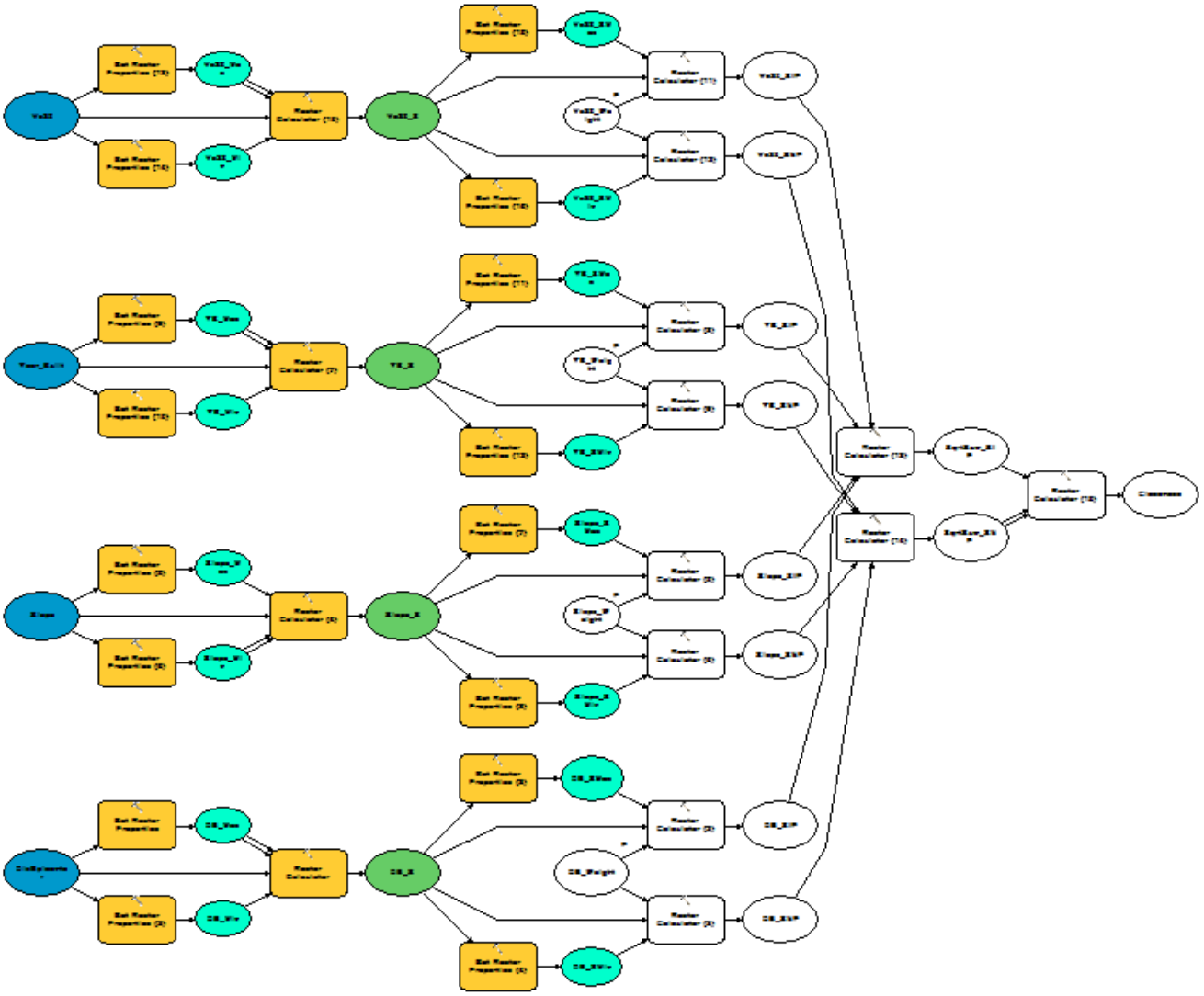

Local TOPSIS ArcGIS Model

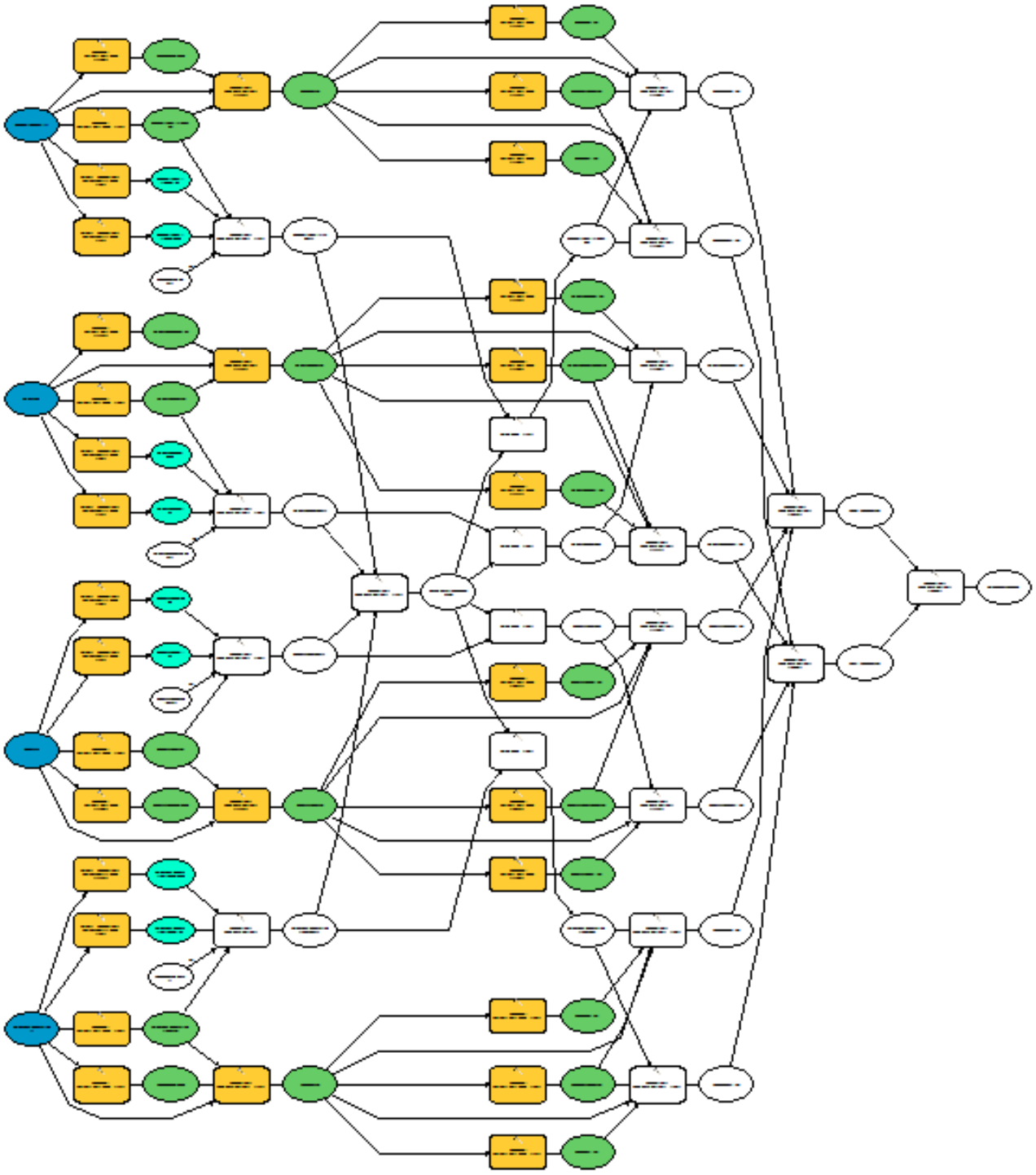

Python script that was used to rank the closeness to ideal point values

```
# Created by: Dr. S. Boroushaki
# Description: Create a Ratser showing the rank values of input raster celss

# import arcpy site-package and os module
import arcpy, os
import numpy as np

# Set geoprocessing environment: a) set  the workspace environment
aWS = r"G:\UNI-GIS\Thesis\Data\Global_TOPSIS.gdb"
arcpy.env.workspace = aWS

# Set geoprocessing environment: b) the overwriteOutput parameter controls whether tools will automatically overwrite any existing output
arcpy.env.overwriteOutput = False

try:
    inRaster = "Closeness_GT"

    # Create a Raster Object and get its lowerleft and cellsize
    aRObject = arcpy.Raster(inRaster)
    lowerLeft = arcpy.Point(aRObject.extent.XMin,aRObject.extent.YMin)
    arcpy.env.outputCoordinateSystem = aRObject.spatialReference
    arcpy.env.extent = aRObject.extent


    # Create a numpy array of the Raster Object
    anArray = arcpy.RasterToNumPyArray(aRObject)

    # Create two arrays:i) unique values and indecies of unique values
    u,indices  = np.unique(anArray,return_inverse=True)
    aRank = (indices.max() - indices +1).reshape(anArray.shape)

    # Convert data block back to raster
    aRankedR = arcpy.NumPyArrayToRaster(aRank, lowerLeft, aRObject.meanCellWidth, aRObject.meanCellHeight, aRObject.noDataValue)

    # Check for existence of data before saving
    if not arcpy.Exists("Ranked"):
        aRankedR.save("Ranked")
    else:
        print "the dataset esxists!"

    # Release raster objects from memory
    del aRObject
    del aRankedR

except ValueError:

    # Code to run when an error occured
    print "An ERROR Occured!"
    print "\n" + arcpy.GetMessages(2)
    del aRObject
    del aRankedR

else:

    # Message when there was no error
    print "\nNo Error occurred"

# Script end message
print "\nEnd of the script!"
```